frontiers in Microbiology

ORIGINAL RESEARCH
published: 09 June 2021
doi: 10.3389/fmicb.2021.636145

The Energetic Potential for Undiscovered Manganese Metabolisms in Nature

Douglas E. LaRowe[1], Harold K. Carlson[1] and Jan P. Amend[1,2]*

[1] Department of Earth Sciences, University of Southern California, Los Angeles, CA, United States, [2] Department of Biological Sciences, University of Southern California, Los Angeles, CA, United States

Microorganisms are found in nearly every surface and near-surface environment, where they gain energy by catalyzing reactions among a wide variety of chemical compounds. The discovery of new catabolic strategies and microbial habitats can therefore be guided by determining which redox reactions can supply energy under environmentally-relevant conditions. In this study, we have explored the thermodynamic potential of redox reactions involving manganese, one of the most abundant transition metals in the Earth's crust. In particular, we have assessed the Gibbs energies of comproportionation and disproportionation reactions involving Mn^{2+} and several Mn-bearing oxide and oxyhydroxide minerals containing Mn in the +II, +III, and +IV oxidation states as a function of temperature (0–100°C) and pH (1–13). In addition, we also calculated the energetic potential of Mn^{2+} oxidation coupled to O_2, NO_2^-, NO_3^-, and FeOOH. Results show that these reactions—none of which, except O_2 + Mn^{2+}, are known catabolisms—can provide energy to microorganisms, particularly at higher pH values and temperatures. Comproportionation between Mn^{2+} and pyrolusite, for example, can yield 10 s of kJ (mol Mn)$^{-1}$. Disproportionation of Mn^{3+} can yield more than 100 kJ (mol Mn)$^{-1}$ at conditions relevant to natural settings such as sediments, ferromanganese nodules and crusts, bioreactors and suboxic portions of the water column. Of the Mn^{2+} oxidation reactions, the one with nitrite as the electron acceptor is most energy yielding under most combinations of pH and temperature. We posit that several Mn redox reactions represent heretofore unknown microbial metabolisms.

Keywords: thermodynamics, bioenergetics, comproportionation, disproportionation, redox reactions

OPEN ACCESS

Edited by:
Hans Karl Carlson, Lawrence Berkeley National Laboratory, United States

Reviewed by:
John D. Coates, University of California, Berkeley, United States
Martial Taillefert, Georgia Institute of Technology, United States
Anirban Chakraborty, University of Calgary, Canada

****Correspondence:***
Douglas E. LaRowe
larowe@usc.edu

Specialty section:
This article was submitted to Microbiological Chemistry and Geomicrobiology, a section of the journal Frontiers in Microbiology

Received: *01 December 2020*
Accepted: *03 May 2021*
Published: *09 June 2021*

Citation:
LaRowe DE, Carlson HK and Amend JP (2021) The Energetic Potential for Undiscovered Manganese Metabolisms in Nature. Front. Microbiol. 12:636145. doi: 10.3389/fmicb.2021.636145

INTRODUCTION

Identifying the catabolic reactions that microorganisms catalyze in nature is critical to understanding the flows of energy and matter in ecosystems. Quantifying the amount of energy available from redox reactions among chemical species reveals which metabolisms could be operating. Gibbs energy calculations have been used in this way to survey the catabolic potential of a number of different ecosystems, such as terrestrial geothermal springs (Inskeep et al., 2005; Shock et al., 2005, 2010; Spear et al., 2005a,b; Windman et al., 2007; Vick et al., 2010; Berenguer, 2011; Cardace et al., 2015), deep-sea hydrothermal systems (Shock et al., 1995; McCollom and Shock, 1997; McCollom, 2000, 2007; Shock and Holland, 2004; Hentscher and Bach, 2012;

Eecke et al., 2013; Dahle et al., 2015; Reed et al., 2015; McKay et al., 2016; Shibuya et al., 2016; Sylvan et al., 2017), shallow-sea hydrothermal systems (Amend et al., 2003, 2011; Rogers and Amend, 2005, 2006; Akerman et al., 2011; Boettger et al., 2013; LaRowe et al., 2014; Han and Perner, 2015; Price et al., 2015; Lu et al., 2020), marine sediments (LaRowe and Regnier, 2008; Schrum et al., 2009; Wang et al., 2010; LaRowe and Amend, 2014, 2015b; Teske et al., 2014; Kiel Reese et al., 2018), the terrestrial subsurface (Osburn et al., 2014), and marine basement rocks (Bach and Edwards, 2003; Edwards et al., 2005). These studies have shown that the energetics of redox reactions are fundamentally constrained by the nature of the compounds and the physiochemical properties of the environment, such as temperature, pressure, and chemical composition. In addition to revealing which catabolic strategies are potentially being used in an environment, Gibbs energy calculations reveal how much energy can be obtained from these reactions and therefore how many cells could be supported by them (Bach and Edwards, 2003; McCollom and Amend, 2005; Amend et al., 2013; LaRowe and Amend, 2014, 2015a,b, 2016; Bach, 2016; Bradley et al., 2018a,b, 2019, 2020).

Similar types of Gibbs energy calculations have been used to predict the existence of novel catabolic strategies that were later found in natural systems and built environments, such as anaerobic ammonia oxidation (anammox) (Broda, 1977; van de Graaf et al., 1995; Kuypers et al., 2003), the anaerobic oxidation of methane (AOM) (Barnes and Goldberg, 1976; Hinrichs et al., 1999; Boetius et al., 2000; Orphan et al., 2001) and complete ammonia oxidation (comammox) (Costa et al., 2006; Daims et al., 2015; van Kessel et al., 2015). Motivated by these successful thermodynamic prognostications, sulfur comproportionation, a heretofore undiscovered catabolic pathway, has recently been predicted to exist in ecosystems with acidic pH over a broad range of temperatures (Amend et al., 2020). These examples show that reactions among compounds formed from elements that have several oxidation states, such as N an S, are candidates for discovering novel catabolic strategies. Here, we have explored the energetic potential of a variety of undiscovered manganese-based microbial metabolisms including comproportionation, disproportionation, and oxidation by several electron acceptors including O_2, NO_2^-, NO_3^-, and FeOOH, summarized schematically in **Figure 1**, as a function of temperature and pH. Redox reactions involving manganese-bearing compounds are likely candidates for novel catabolic strategies due to the ubiquity of Mn in Earth's crust and the large number of microbial species that can enzymatically reduce and oxidize compounds containing it, as reviewed below. In this manuscript, we calculate the impact of temperature, pH and other compositional variables on the Gibbs energy of Mn redox reactions that could support microbial activities.

Manganese in the Earth System

Mn oxides are found in ocean and lake sediments, ore deposits, soils, hydrothermal vents (Villalobos et al., 2003; Yang et al., 2018), interlayered with Fe-oxides that have recently become aerobic (Tazaki, 2000), caves (Northup et al., 2003) streams, and desert varnish (Tebo et al., 2004). Aqueous Mn(II), Mn^{2+}, is common in suboxic and anoxic settings such as sediment pore water (Madison et al., 2013; Oldham et al., 2017b), stratified water bodies (Trouwborst et al., 2006; Yakushev et al., 2007, 2009; Dellwig et al., 2012; Oldham et al., 2015), ground water (Wasserman et al., 2006; de Meyer et al., 2017; McMahon et al., 2019) and drinking water systems (Cerrato et al., 2010). Mn(II) often coexists with birnessite (δ-MnO_2) where redox conditions fluctuate, such as in ocean and lake sediments (Yang et al., 2018). The presence of aqueous Mn(III) in natural systems has recently become more appreciated, e.g., (Trouwborst et al., 2006; Madison et al., 2011, 2013; Oldham et al., 2015, 2017a,b), and in some settings, aqueous Mn(III) can constitute all or nearly all of the aqueous pool of dissolved Mn (Madison et al., 2011; Oldham et al., 2015, 2017b). Since aqueous Mn^{3+} rapidly disproportionates (Davison, 1993), aqueous Mn(III) is thought to be complexed to ligands that stabilize it, likely organic compounds (Heintze and Mann, 1947; Klewicki and Morgan, 1998; Parker et al., 2004; Duckworth and Sposito, 2005). Furthermore, trivalent Mn can also be stabilized in solid phase such as MnOOH through comproportionation reactions (Tu et al., 1994; Mandernack et al., 1995; Bargar et al., 2005; Elzinga, 2011, 2016; Elzinga and Kustka, 2015; Hinkle et al., 2016; Zhao et al., 2016; Wang et al., 2018), including during bacterial Mn(IV) reduction (Johnson et al., 2016). Finally, it is noteworthy, that unlike Fe in many settings, dissolved Mn passes through a 0.02 micron filter, indicating that it is actually an aqueous species, not part of a colloid (Oldham et al., 2017b). See **Table 1** for a selection of environments in which Mn concentrations in natural settings have been reported.

Microbial Processing of Manganese

Microorganisms can reduce and oxidize Mn compounds to gain energy. Though no obligate Mn-reducers are known, the biological reduction of Mn-oxides to Mn^{2+} has been shown to occur in a number of environments (Burdige and Nealson, 1985; Lovley and Phillips, 1988; Myers and Nealson, 1988; Tebo et al., 1991; Burdige et al., 1992; Burdige, 1993; Gounot, 1994; Henkel et al., 2019). Microbial Mn(II) oxidation is phylogenetically widespread, occurring in bacteria, archaea, and eukarya (Hansel, 2017), and the enzymes associated with this process are diverse (Wright et al., 2018). A community of microorganisms has even been shown to photooxidize Mn^{2+} under anoxic conditions (Daye et al., 2019). Taken together, Mn^{2+} oxidation is thought to be responsible—directly or by environmental modification—for the formation of the majority of Mn oxides in nature (Tebo et al., 2004). Although this process has been well-studied, e.g., (Nealson et al., 1988; Tebo et al., 2004; Hansel, 2017), it was only recently shown that a microorganism can catalyze Mn^{2+} oxidation to gain energy (Yu and Leadbetter, 2020). It has also been demonstrated that microorganisms can reduce aqueous ligand-bound Mn(III) (Kostka et al., 1995; Szeinbaum et al., 2014, 2017, 2020) and solid-phase Mn(III), in the form of manganite (MnOOH) (Larsen et al., 1998; Fredrickson et al., 2002), to provide energy for microorganisms.

Mn oxidation and reduction are known to take place simultaneously in the same system, and there are isolates known that can both reduce and oxidize Mn, e.g., *Lysinibacillus*

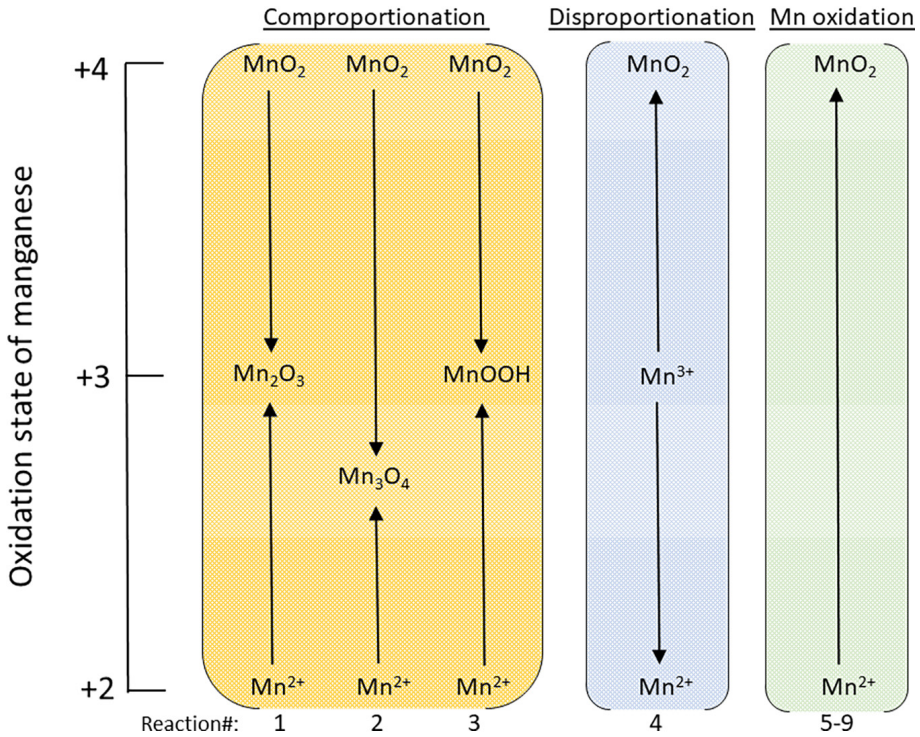

FIGURE 1 | Schematic illustrating how the oxidation state of manganese changes for the comproportionation, disproportionation and Mn^{2+} oxidation reactions considered in this study. The reactions numbers at the bottom of the figure correspond to the reactions in **Table 3**. The oxidation state of hausmannite, Mn_3O_4, is shown as 2.67, the average for Mn in this phase: $Mn^{II}(Mn^{III})_2O_4$.

fusiformis, *Bacillus pumilus*, and *B. cereus* (Cerrato et al., 2010). Phylogenetic studies of iron-manganese nodules on the seafloor have shown that the associated microbial communities are significantly distinct from those in surrounding sediments and that the interior communities are different from the exteriors of these nodules, suggesting that more diversity on the interior could indicate Mn cycling (Tully and Heidelberg, 2013). A metagenomic study on ferromanganese crusts on Takuyo-Daigo Seamount found putative genes for dissolution and precipitation of Mn, including protein-coding DNA sequences similar to outer-membrane *c*-type cytochromes that *Shewanella* spp. use to reduce Mn(IV) and protein-coding DNA sequences similar to Mn oxidases such as MopA and multicopper oxidase sequences (Kato et al., 2019). In shallower ocean settings, Mn^{2+} can be found with layered Mn-oxides when Mn^{2+} diffuses upward in sediments into oxic zones (Yang et al., 2018). Microfossil evidence in ferromanganese nodules and crusts support the notion that microbial activity is responsible for concentrating Mn in nodules and crusts from seawater (Jiang et al., 2019), where Mn concentration is typically 0.1–0.15 nm (van Hulten et al., 2017). Similarly, nodules from the NE Equatorial Pacific were revealed to have connected pore space and molecular data showed that the microbial community was dominated by nodule-specific Mn(IV)-reducing and Mn(II)-oxidizing bacteria that were not found in the surrounding environment (Blöthe et al., 2015).

MATERIALS AND METHODS

Values of overall Gibbs energies at the conditions of interest, ΔG_r, are calculated using:

$$\Delta G_r = \Delta G_r^0 + RT\ln Q_r \quad (1)$$

where ΔG_r^0 and Q_r refer to the standard molal Gibbs energy and the reaction quotient of the indicated reaction, respectively, R represents the gas constant, and T denotes temperature in Kelvin. Values of ΔG_r^0 were calculated using the revised-HKF equations of state (Helgeson et al., 1981; Tanger and Helgeson, 1988; Shock et al., 1992), the SUPCRT92 software package (Johnson et al., 1992), and thermodynamic data taken from a number of sources (Robie and Bethke, 1963; Bricker, 1965; Helgeson et al., 1978; Hem et al., 1982; Robie and Hemingway, 1985; Shock and Helgeson, 1988; Shock et al., 1997; Chase, 1998; Senoh et al., 1998; Schulte et al., 2001; Snow et al., 2013; LaRowe and Amend, 2014; see **Table 2**). Values of Q_r are calculated using:

$$Q_r = \prod_i a_i^{\nu_i}, \quad (2)$$

where a_i stands for the activity of the ith species and ν_i corresponds to the stoichiometric coefficient of the ith species in the reaction of interest. Negative values of ΔG_r are said to be exergonic and positive values are endergonic; $\Delta G_r = 0$ defines equilibrium. Because standard states in thermodynamics specify

TABLE 1 | Concentration of Mn in selected environmental settings.

Environment	Species or phase	Concentration	References
Black Sea water column (various depths)	Dissolved Mn	0.49–2.15 μmol L^{-1}	Clement et al., 2009
	Particulate Mn-oxides	0.01–1.4 μmol L^{-1}	
Chesapeake Bay water column	Particulate Mn-oxide	0–4.89 μmol L^{-1}	Oldham et al., 2015
	Mn(II),aq	0.59–8.04 μmol L^{-1}	
	Mn(III),aq	0–6.98 μmol L^{-1}	
North Atlantic Water Column	Particulate Mn oxides	0.19–3.5 nmol L^{-1}	Jones et al., 2020
	Mn(III)-ligand, aq	0.01–0.83 nmol L^{-1}	
	Mn(II), aq	0.5–25 nmol L^{-1}	
Oneida Lake bottom water	Mn(II), aq	0.48–3.3 μmol L^{-1}	Chapnick et al., 1982
Mouth/Lower St. Lawrence Estuary sediment	Mn Oxide	0 –130 μmol g^{-1}	Madison et al., 2013
	Mn(II), aq	0–200 μmol L^{-1}	
	Mn(III), aq	0–70 μmol L^{-1}	
Amazon fan sediment	Mn(II)	3.2 g Mn (kg sediment)$^{-1}$	Kasten et al., 1998
Fe-Mn nodule-rich marine sediment pore water	Mn(II)	0–38 μmol L^{-1}	de Lange et al., 1992
Various Fe-Mn Nodules	Mn	15.9–34.2 weight %	Hein, 2013
Swiss lake sediment porewater	Shallow water Mn, aq	10–30 μmol L^{-1}	Schaller and Wehrli, 1996
	Deep water Mn, aq	110–350 μmol L^{-1}	
Groundwater in China	Mn, aq	0–62.1 μmol L^{-1}	Hou et al., 2020
Groundwater in Scotland	Mn, aq	0–35 μmol L^{-1}	Homoncik et al., 2010
Groundwater in the United States	Mn,aq	0–20,630 μmol L^{-1}	McMahon et al., 2019
Drinking water, rural Bangladesh	Mn, aq	2-100 μmol L^{-1}	Akter et al., 2016
Hydrothermal vent plumes, Juan de Fuca Ridge	Dissolved Mn	0–∼600 nmol L^{-1}	Chin et al., 1994
Hydrothermal plume and surrounding bottom water, Galapagos Rift	Total dissolvable Mn	0.41–24 μg per kg	Klinkhammer et al., 1977
San Clemente Basin sediment (near cold seep)	Dissolved Mn	0–∼600 μmol L^{-1}	McQuay et al., 2008
Atlantic pelagic sediment pore water	Mn(II)	0–100 μmol L^{-1}	Froelich et al., 1979
River Leie sediment pore water, Menen Belgium	Total Dissolved Mn	3.77–39.1 μmol L^{-1}	Gao et al., 2007
Zambezi fan sediment	Mn(II)	∼2–12 μmol L^{-1}	März et al., 2008
	Solid Mn	∼0.3–∼0.4 g/kg	
German tidal wetlands (median)	Dissolved Mn	8.4 μmol L^{-1}	Hamer et al., 2020

a composition and state of aggregation (Amend and LaRowe, 2019; LaRowe and Amend, 2020) values of Q_r must be calculated to take into account how environmental conditions impact Gibbs energy calculations. In this study we use the classical chemical-thermodynamic standard state in which the activities of pure liquids and solids are taken to be 1 as are those for aqueous species in a hypothetical 1 molal solution referenced to infinite dilution at any temperature or pressure. Additional information detailing how the Gibbs energy calculations were carried out can be seen in the **Supplementary Materials**.

Activities are related to concentration, C, by

$$a_i = \gamma_i \left(\frac{C_i}{C_i^{\Theta}} \right) \tag{3}$$

where γ_i and C_i stand for the individual activity coefficient and concentration of the ith species, respectively, and C_i^{θ} refers to the concentration of the ith species under standard state conditions, which is taken to be equal to one molal referenced to infinite dilution. Values of γ_i can be computed using an extended version of the Debye–Hückel equation (Helgeson, 1969). Values of γ_i vary, mostly, as a function of temperature, ionic strength and charge. For reference, γ_i for Mn^{2+} in seawater at 25°C and 1 bar is 0.16. Therefore, $a_{Mn^{2+}} = 10^{-6}$ corresponds to a concentration of 6.25 μmol (kg H_2O)$^{-1}$ under these conditions. For other temperatures, charge states and ionic strengths, see Amend and LaRowe (2019) for values of γ_i.

The calculations summarized in the figures discussed below have been carried out over a range of plausible natural conditions (see **Table 1**). We have focused on pH, $-\log a_{H^+}$, because it tends to be a master variable in natural settings and it can vary by many orders of magnitude, thereby significantly altering the energetic potential of a reaction that has hydrogen ions in it. The activities of the other aqueous species, O_2, NO_2^-, NO_3^-, N_2, NH_4^+, Mn^{2+}, and Mn^{3+}, tend to vary less than H^+. Their activities are meant to be representative of common natural settings. To illustrate the impact of variable Mn^{2+} activities, we have also calculated the Gibbs energies of two reactions, those with the largest and smallest stoichiometric numbers for Mn^{2+}, as a function of $a_{Mn^{2+}}$. The Gibbs energies of Mn^{2+} oxidation by O_2 is included in this analysis as a basis of comparison for the other Mn^{2+} oxidation reactions as well as because it has only recently been shown to support the energetic needs of an organism under one set of compositional conditions (Yu and Leadbetter, 2020).

Although the thermodynamic data required to calculate the Gibbs energies of Mn-oxides as a function of temperature have been available for decades, they have not been presented in a

TABLE 2 | Summary of the standard molar thermodynamic properties at 25°C and 1 bar and heat capacity power function coefficients (*a*, *b*, and *c*) for selected Mn-bearing minerals.

Compound	Formula	ΔG_f^{0a}	ΔH_f^{0a}	S^{0b}	V^{0c}	a^d	b^e	c^f	T_{max}/T_{range} (K)
Pyrolusite	MnO_2	−465,000[g]	−520,000[h]	52.75[h]	16.61[i]	51.47[i]	42.78[i]	−8.368[i]	1,000
Bixbyite	Mn_2O_3	−882,100[g]	−959,000[h]	113.7[h]	31.38[i]	−67.51[i]	521.7[i]	19.36[i]	240–300
						217.2[i]	−355[i]	0j	300–325
						101.4[i]	36.59[i]	−11[i]	325–1,400
Hausmannite	Mn_3O_4	−1,279,000[g]	−1,384,500[h]	165.60[h]	46.96[i]	149.5[i]	52.75[i]	−20.02[i]	270–1,100
Feitknechtite	β-MnOOH	−543,100[k]							
Nsutite	γ-MnO_2	−456,500[l]							
Manganite	γ-MnOOH	−557,700[l]							
Birnessite	δ-MnO_2	−453,100[l]							
Pyrochroite	$Mn(OH)_2$	−615,630[l]							
Amorphous $Mn(OH)_2$	$Mn(OH)_2$	−615,000[m]							

[a] *J mol*$^{-1}$; [b] *J K*$^{-1}$ *mol*$^{-1}$; [c] *cm*^{3} *mol*$^{-1}$; [d] *J mol*$^{-1}$; [e] 10^3 *J K*$^{-2}$ *mol*$^{-1}$; [f] 10^{-5} *J K mol*$^{-1}$; [g] *calculated from* ΔH^0 *and* S^0 *and* S^0 *of the elements taken from Chase (1998);* [h] *Robie and Hemingway (1985);* [i] *Robie and Bethke (1963);* [j] *calculated by regressing isobaric heat capacity data as a function of temperature from h using the Maier–Kelly equation (see section "Materials and Methods");* [k] *Hem et al. (1982);* [l] *Bricker (1965);* [m] *Senoh et al. (1998).* T_{max}/T_{range} *refers to, respectively, the maximum temperature and temperature range to which the thermodynamic data are valid.*

TABLE 3 | Manganese catabolic reactions considered in this study.

Comproportionation reactions

1 $MnO_2 + Mn^{2+} + H_2O \rightarrow Mn_2O_3 + 2H^+$

2 $MnO_2 + 2Mn^{2+} + 2H_2O \rightarrow Mn_3O_4 + 4H^+$

3 $MnO_2 + Mn^{2+} + 2H_2O \rightarrow 2MnOOH + 2H^+$

Disproportionation reaction

4 $2Mn^{3+} + 2H_2O \rightarrow MnO_2 + Mn^{2+} + 4H^+$

Mn oxidation reactions

5 $2Mn^{2+} + O_{2(aq)} + 2H_2O \rightarrow 2MnO_2 + 4H^+$

6 $3Mn^{2+} + 2NO_2^- + 2H_2O \rightarrow 3MnO_2 + N_{2(aq)} + 4H^+$

7 $4Mn^{2+} + NO_3^- + 5H_2O \rightarrow 4MnO_2 + NH_4^+ + 6H^+$

8 $5Mn^{2+} + 2NO_3^- + 4H_2O \rightarrow 5MnO_2 + N_{2(aq)} + 8H^+$

9 $Mn^{2+} + 6FeOOH \rightarrow MnO_2 + 2Fe_3O_4 + 2H_2O + 2H^+$

The following chemical formulas refer to the indicated crystalline Mn phases: MnO_2 *(pyrolusite),* Mn_2O_3 *(bixbyite),* Mn_3O_4 *(hausmannite), MnOOH (manganite and feitknechtite), FeOOH (2-line ferrihydrite), and* Fe_3O_4 *(magnetite).*

format amenable to commonly used thermodynamic software such as SUPCRT, OBIGT, EQ3/6, and CHNOSZ [see Dick (2019) and chnosz.net for a discussion of thermodynamic databases]. Consequently, these data are presented along with the parameters used to calculate thermodynamic variables as a function of temperature, as regressed using the Maier–Kelly equation (Maier and Kelley, 1932), in **Table 2** (i.e., the *a*, *b*, and *c* parameters). The thermodynamic properties of pyrolusite (MnO_2) are used in the Gibbs energy calculations in place of the more commonly abundant birnessite (δ-MnO_2) because the thermodynamic properties for pyrolusite are known as a function of temperature and those for birnessite are not. As can be seen in **Table 2**, there is a 2.6% difference in the Gibbs energies of formation for these two phases at 25°C and 1 bar.

RESULTS

Values of the overall Gibbs energies, ΔG_r, of the reactions listed in **Table 3**, hereafter referred to by the reaction numbers in this table only, are shown as a function of pH in **Figures 2–4** from 0 to 100°C with the exception of the comproportionation reactions involving both MnOOH phases (**Figure 2C**, Reaction 3), which are shown only at 25°C, the extent of the thermodynamic data for these phases. Since the hydrogen ion is on the right side of all of the reactions considered in this communication, values of ΔG_r become more negative and thus more favorable as pH increases. In general, Mn reactions are more exergonic at higher temperatures than lower ones, particularly as pH values increase. The activities of several species are fixed at the values noted in each figure caption to reduce the number of figures to a comprehensible total. The impact of varying these activities on Gibbs energies of reactions is proportional to the stoichiometric coefficients in front of them, as per Equation 2. Values of ΔG_r for the Mn^{2+} oxidation reactions are reported in units of kJ (mol e^-)$^{-1}$ to facilitate comparison amongst these reactions as well as other such reactions reported in the literature that also use these units (see section "Introduction"). It is clear how many electrons are transferred between reactants and products in these reactions [e.g., Mn^{2+} oxidation to MnO_2 represents a two electron transfer; Mn(II) becomes Mn(IV)]. However, units of kJ (mol Mn)$^{-1}$ are used for the comproportionation and disproportionation reactions because the average oxidation state of Mn is the same on both sides of these reactions, obfuscating how the number of electrons transferred in the process should be counted. This follows how the Gibbs energies were reported for a number of fermentation (i.e., disproportionation) reactions (LaRowe and Amend, 2019).

The impact of Mn^{2+} activities on the Gibbs energies of Reactions 8 and 9 are plotted in **Figures 5A,C** from 0 to 100°C at pH 7. Since Mn^{2+} is on the left-hand side of these reactions, increasing activities of Mn^{2+} results in lower values of ΔG_r for all temperatures. In the case of nitrate reduction, Reaction 8, Gibbs energies at 25°C decrease from −1.8 kJ (mol e^-)$^{-1}$ at $a_{Mn^{2+}} = 10^{-9}$ to −18.9 kJ (mol e^-)$^{-1}$ at $a_{Mn^{2+}} = 10^{-3}$. By comparison, ΔG_r for Reaction 9, ferrihydrite reduction, drops

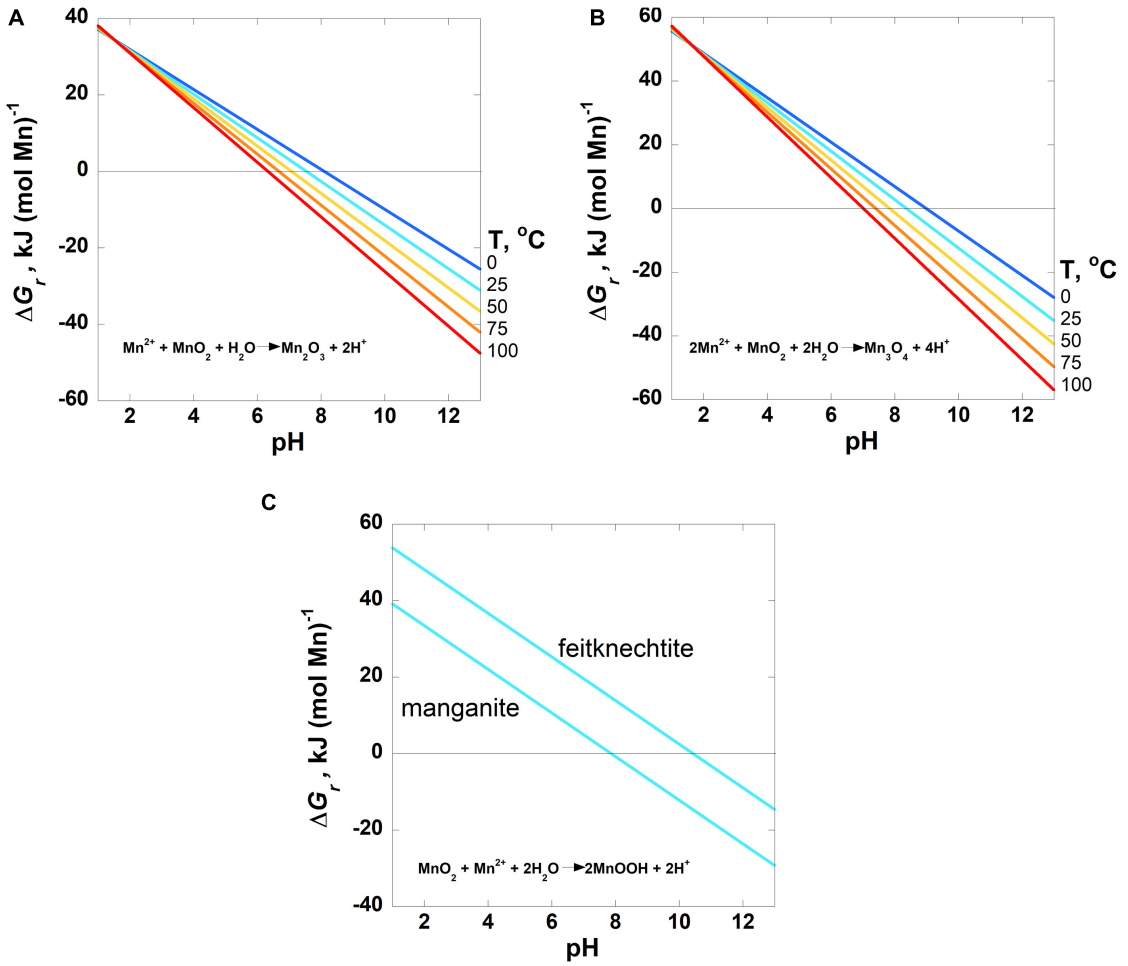

FIGURE 2 | Overall Gibbs energies, ΔG_r, of the comproportionation reactions listed in **Table 3** (Reactions 1–3) as a function of pH from 0 to 100°C for **(A)** bixbyite and **(B)** hausmannite formation and **(C)** at 25°C for MnOOH, manganite and feitknechtite, formation. For all three reactions, the activity of $Mn^{2+} = 10^{-6}$. Activities of H_2O and all solid phases are taken to be 1. The horizontal line in each panel designates where $\Delta G_r = 0$; Gibbs energies below this line are exergonic.

from 11.6 to −5.5 kJ (mol e^-)$^{-1}$ over the same $a_{Mn}{}^{2+}$ range at 25°C. The impact of Mn activities is only shown for two reactions to illustrate the relative impact of this variable on reaction energetics. The particular reactions chosen are those that have the largest and smallest stoichiometric numbers for Mn^{2+}, and therefore values of ΔG_r that are the most and least sensitive to Mn^{2+} activities (see Equations 1, 2).

The Gibbs energies of three comproportionation reactions among pyrolusite and Mn^{2+}, forming bixbyite (Mn_2O_3), hausmannite (Mn_3O_4) and two manganese oxyhydroxide phases (MnOOH–manganite and feitknechtite), were considered in this study (see Reactions 1–3; **Figure 2A**) along with one disproportionation reaction (Reaction 4; **Figure 3**). The results are normalized to units of kJ (mol Mn)$^{-1}$. The comproportionation reactions forming bixbyite and hausmannite are exergonic at ∼pH > 6 at 100°C. Higher pHs are necessary at lower temperatures for these reactions to be favored: pH ∼7 at 50°C and pH ∼8 at 0°C. The comproportionation reactions forming manganite and feitknechtite, shown in **Figure 2C**, are exergonic above pH 8 and 10, respectively, at 25°C. In contrast to these comproportionation reactions, the disproportionation of Mn^{3+} to Mn^{2+} and pyrolusite (Reaction 4; **Figure 3**), is exergonic from 0–100°C throughout the pH range considered. At all pH values, Gibbs energies are lower (more favorable) for Reaction 4 as temperatures increase. In addition, the values of ΔG_r for this reaction are three to six times more exergonic than the disproportionation reactions.

The energetic potentials of Mn^{2+} oxidation by $O_{2(aq)}$, NO_2^-, NO_3^- and 2-line ferrihydrite (FeOOH) (Reactions 5–9) are shown in the panels in **Figure 4** as a function of temperature and pH for the indicated activities of the aqueous species in each reaction. Slightly different from Reactions (1–4) in **Figures 2**, **3**, the results of these reactions are shown per mole of electron transferred. The reduction of oxygen (Reaction 5, **Figure 4A**) is exergonic at all temperatures for pH values above ∼3.7, varying slightly with temperature. Values of ΔG_r for Reaction 6, in which nitrite is the oxidant, are

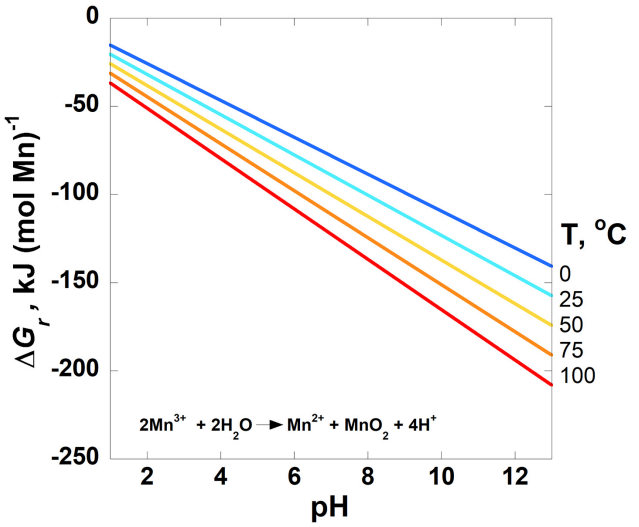

FIGURE 3 | Overall Gibbs energies, ΔG_r, of the disproportionation reaction given in **Table 3** (Reaction 4) as a function of pH from 0 to 100°C for pyrolusite formation. The activities of Mn^{2+} and Mn^{3+} are set to 10^{-6}. Activities of H_2O and all solid phases are taken to be 1. The horizontal line designates where $\Delta G_r = 0$; Gibbs energies below this line are exergonic.

exergonic throughout nearly the entire pH and temperature range considered, with the only exceptions being at 75 and 100°C below pH 2 (**Figure 4B**). **Figures 4C,D** both show the Gibbs energies of Mn^{2+} oxidation with nitrate (Reactions 7 and 8), but differ in the oxidation state of the nitrogen product species (NH_4^+ and N_2, respectively). The major difference between these reactions is that the complete reduction of NO_3^- to NH_4^+ is less exergonic per electron transferred than the partial reduction to N_2. Reaction 8 (N_2 formation) becomes exergonic from about pH 6–7, depending on temperature, while Reaction 7 (NH_4^+ formation) does not become favorable until about pH 9.5–12, from 100 to 0°C. Finally, values of ΔG_r for the oxidation of Mn^{2+} coupled to the reduction of FeOOH (Reaction 9; **Figure 4E**) become exergonic over a pH range of 6–8, depending on temperature.

The standard state Gibbs energies, ΔG_r^0, of Reactions 1, 2, 3, 7, 8, and 9 are shown as a function of temperature in **Figure 6**. This subset of reactions is illustrated because $\Delta G_r^0 > 0$ for all of them at all temperatures except above 95°C for Reaction 8. In fact, values of the standard state Gibbs energies for each of these reactions, except Reaction 8, are greater than 20 kJ $(\text{mol } e^-)^{-1}$ or $(\text{mol Mn})^{-1}$. Both sets of units appear on the y-axis since the comproportionation and disproportionation reactions are normalized per mole of Mn and the oxidation reactions are normalized per mole of electron transferred.

Four other oxidants were also considered in possible oxidation reactions of Mn^{2+} to pyrolusite (CO to CH_4; NO_3^- to NO_2^-; magnetite to Fe^{2+}; ferrihydrite to Fe^{2+}), but none of these reactions was exergonic over a broad range of temperature, pH, and other compositional conditions (not shown).

DISCUSSION

The calculations presented above demonstrate that comproportionation and disproportion reactions involving Mn species, as well as Mn^{2+} oxidation with various electron acceptors, could provide energy for microorganisms. However, these reactions can only be catalyzed by organisms in environments where the composition and temperature allow it. The impact of taking into account non-standard state activities of reactants and products on energy yields is clearly shown in **Figures 2–6**, where standard state and overall Gibbs energies of reactions are compared. Note that values of ΔG_r^0 are positive throughout nearly the entire range of temperatures considered, but those of ΔG_r, which take into account non-standard state compositions, can be negative (i.e., exergonic). Our results illustrate the importance of pH in determining the exergonicity of reactions involving Mn: with the exception of the Mn^{3+} disproportionation reaction (Reaction 4), all of the reactions considered in this study are not thermodynamically favored at low pH. It should be noted that just because a given reaction is exergonic under a particular set of environmental conditions, this does not necessarily mean that organisms will catalyze it. The thermodynamic favorability of reactions indicated by Gibbs energy is a statement of the possible—it quantifies the tendency of a chemical reaction to proceed in a particular direction. Gibbs energy calculations do not reveal the path of a process or information about intermediate species or reactions that might be occurring. However, ΔG_r can still quantify the potential for complex, multi-organism processes such as AOM. The microbial coupling of methane oxidation to sulfate reduction was predicted to exist thermodynamically before it was demonstrated to occur in nature. A large body of research has since shown that AOM is catalyzed by a consortia of microorganisms through a rather complex series of steps that are yet to be fully understood [see Knittel et al. (2019) for a review]. However, because the overall process can be represented by a chemical reaction that accurately describes how chemical species are transformed, the Gibbs energy of the AOM reaction can be used to quantify the amount of energy associated with the overall change. In a similar manner, the Mn reactions considered in this study might not capture the complexity of how organisms in nature might take advantage of them for energy, but as long as the overall process corresponds to the observed mass transfer associated with this reaction, then the Gibbs energies reported in this study are a valid prediction of possible catabolisms and provide a theoretical basis for future research.

Values of Gibbs energies for the reactions shown in **Table 3** are more sensitive to pH than the activity of Mn^{2+}. This is because the stoichiometric numbers in front of H^+ are larger than those in front of Mn^{2+} for any given reaction. The quantitative difference of pH vs. Mn^{2+} activity, $a_{Mn}{}^{2+}$, on values of ΔG_r are shown in **Figure 5**. As noted above, **Figures 5A,C** show ΔG_r for Reactions 8 and 9 as a function of $a_{Mn}{}^{2+}$ at pH 7. **Figures 5B,D** are rescaled versions of **Figures 4D–E**, illustrating Gibbs energies of Reactions 8 and 9 as a function of pH at a $a_{Mn}{}^{2+} = 10^6$. It can be seen in

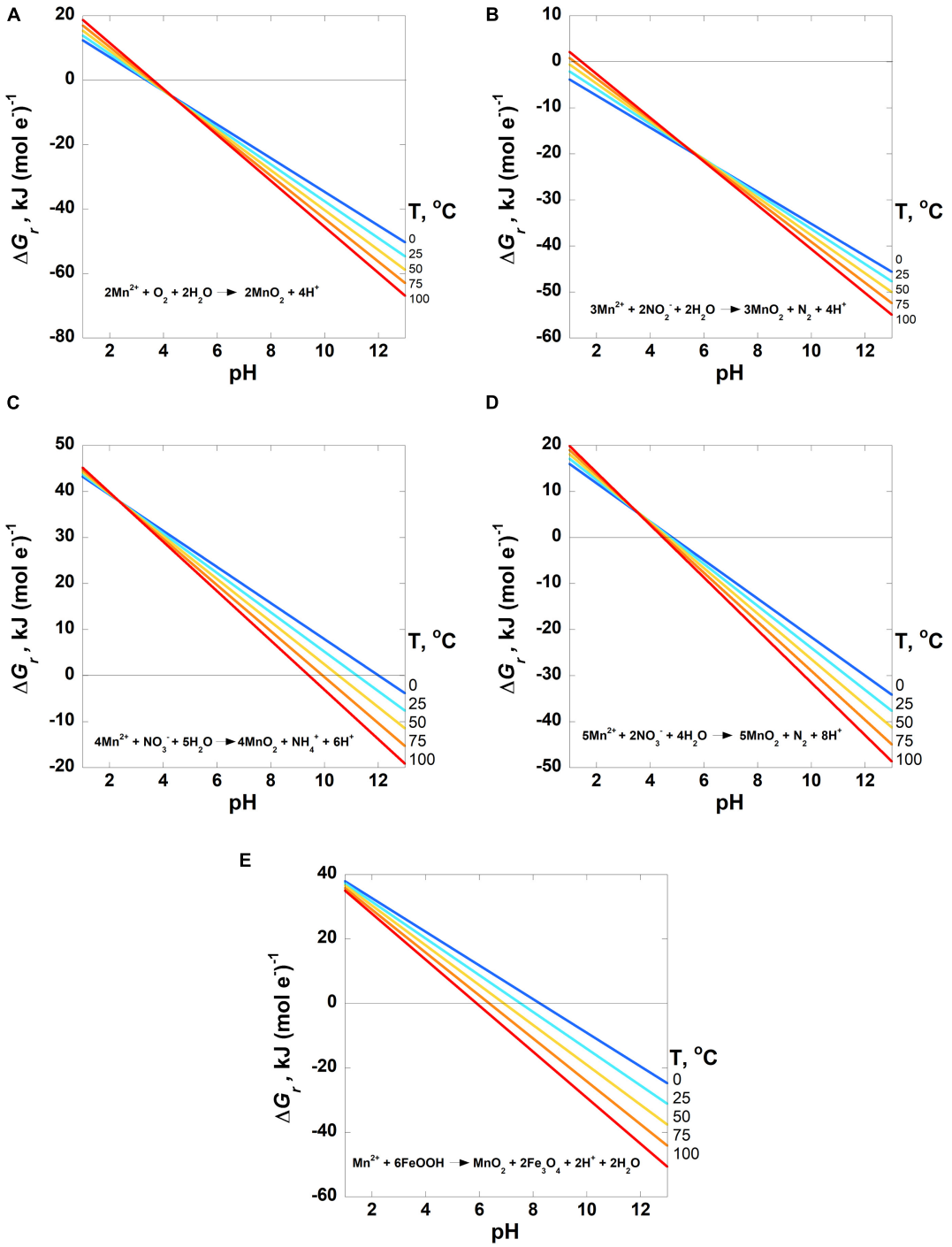

FIGURE 4 | Overall Gibbs energies, ΔG_r, of the Mn^{2+} oxidation reactions listed in **Table 3** [Reactions 5–9 in panels **(A–E)**, respectively] as a function of pH from 0 to 100°C. Activities of H_2O and all solid phases are taken to be 1 and the activity of $Mn^{2+} = 10^{-6}$. The activities of the other species are **(A)** $O_2 = 10^{-4}$; **(B)** $NO_2^- = 10^{-7}$ and $N_2 = 10^{-4}$; **(C)** $NO_3^- = 10^{-5}$ and $NH_4^+ = 10^{-5}$; **(D)** $NO_3^- = 10^{-5}$ and $N_2 = 10^{-4}$. The horizontal line in each panel designates where $\Delta G_r = 0$; Gibbs energies below this line are exergonic.

Figure 5 that the slopes of the lines depicting ΔG_r as a function of pH are steeper and cover a broader range of values than those plotted as a function of $a_{Mn}{}^{2+}$ for the same reaction. For example, Gibbs energies at 25°C for nitrate reduction, Reaction 8, change from −1.8 kJ (mol e^-)$^{-1}$ at $a_{Mn}{}^{2+} = 10^{-9}$ to −18.9 kJ (mol e^-)$^{-1}$ at $a_{Mn}{}^{2+} = 10^{-3}$ (**Figure 5A**). For the same order of magnitude change in pH, values of ΔG_r for the same reaction change from 3.4 kJ (mol e^-)$^{-1}$ at pH 4 to −24.0 kJ (mol e^-)$^{-1}$

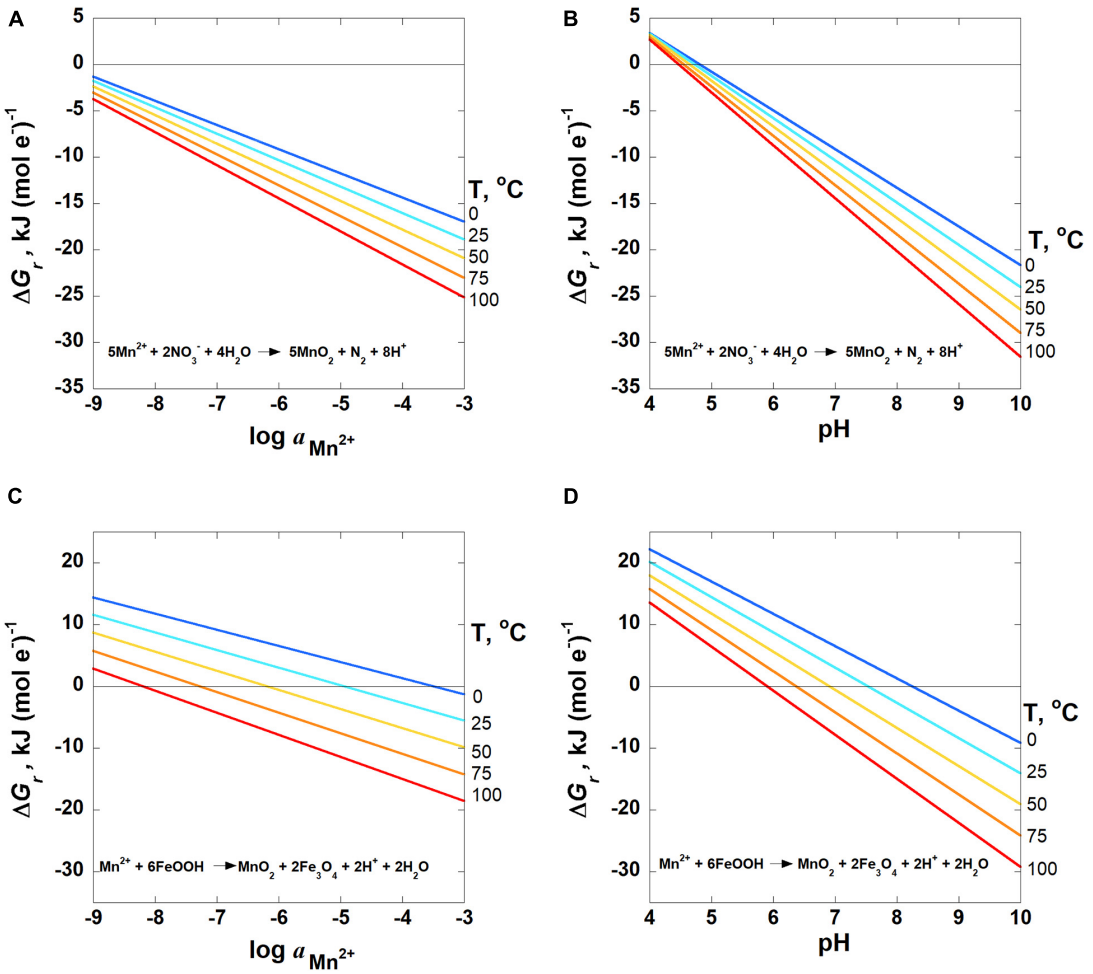

FIGURE 5 | Overall Gibbs energies, ΔG_r, of Reactions **(A,B)** 8 and **(C,D)** 9 as a function of **(A,C)**$\log a_{Mn}^{2+}$ at pH = 7 and **(B,D)** pH for $a_{Mn}^{2+} = 10^{-6}$ from 0 to 100°C. Activities of H_2O and all solid phases are taken to be 1. The activities of N_2 and NO_3^- are 10^{-4} and 10^{-5}, respectively. The horizontal line in each panel designates where $\Delta G_r = 0$; Gibbs energies below this line are exergonic.

at pH 10 (**Figure 5C**). Similarly, ΔG_r for Reaction 9, ferrihydrite reduction, drops from 11.6 kJ (mol e^-)$^{-1}$ to −5.5 (mol e^-)$^{-1}$ over the same six-order of magnitude Mn^{2+} range at 25°C, and from 20.2 kJ (mol e^-)$^{-1}$ to −14.1 kJ (mol e^-)$^{-1}$ from pH 4–10.

The results presented above also illustrate that substantial differences in reaction energetics can correspond to seemingly subtle differences in the identity of reaction products. For example, values of ΔG_r for Reaction 3 differ by ∼15 kJ (mol Mn)$^{-1}$ depending on whether manganite or feitknechtite (both MnOOH) are the reaction product, a point that has been made for analogous Fe-oxyhydroxide species (LaRowe and Amend, 2014). Similarly, we show that the energetics of oxidation of Mn^{2+} by NO_3^-, Reactions 7 and 8, depend dramatically on the identity of the product species formed. As shown in **Figures 4C,D**, when N_2 is the product N species rather than NH_4^+, the values of ΔG_r are far more favorable for the incomplete reduction of NO_3^-, over 30 kJ (mol e^-)$^{-1}$ at all temperatures.

Natural settings that could host the manganese redox reactions noted in this study are widespread. Sediments in general serve as plausible locations for comproportionation, disproportionation and Mn^{2+} oxidation reactions since they can contain coexisting Mn-oxides in particle form and aqueous Mn^{2+} (Luther et al., 1997) and ligand-bound Mn^{3+} in pore fluids (Madison et al., 2011, 2013; see **Table 1**), in addition to multiple oxidants such as oxygen, nitrate (see below), nitrite, and iron hydroxides (Schulz and Zabel, 2006). Disproportionation of Mn^{3+} could also occur in the redox-stratified water bodies where it has been found, such as the Chesapeake Bay (Oldham et al., 2015), the St. Lawrence Estuary (Oldham et al., 2017b), the Black Sea (Trouwborst et al., 2006) and even in oxic portions of the water column (Oldham et al., 2017a). It should be noted that the energetics of reactions involving aqueous ligand-bound Mn(III) species will vary depending on the bond strength between Mn and the ligand, and therefore the identity of the ligand. Comproportionation reactions could occur in nearly any setting where Mn-oxides and appreciable

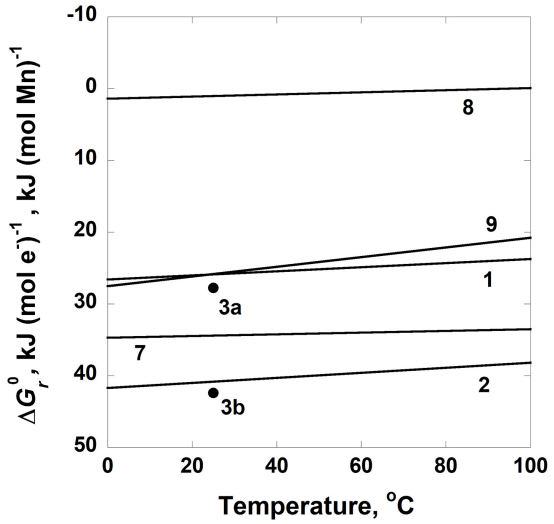

FIGURE 6 | Standard state Gibbs energies, ΔG_r^0, of Reactions 1–3 and 7–9 in **Table 3** as a function of temperature. Units of kJ (mol Mn)$^{-1}$ are given for Reactions 1–3 and kJ (mol e$^-$)$^{-1}$ for Reactions 7–9. The solid circles labeled 3a and 3b refer to values of ΔG_r^0 for Reaction 4 at 25°C where manganite and feitknechtite, respectively, are the phases of MnOOH.

aqueous Mn^{2+} coexist at neutral to high pH. As noted in the introduction, iron-manganese nodules on the seafloor, which are ubiquitous (Orcutt et al., 2020) could be one such location, especially according to the model described by Kato et al. (2019).

In addition to the seafloor and sediments, all of the Mn-based metabolisms considered in this study could be supported in aquifers throughout the world given their relatively large concentrations of aqueous Mn (see **Table 1**) and varying oxidation states. For instance, less than half of groundwater in the United States is considered to be oxic (DeSimone et al., 2015). Add in the fact that roughly one-third of United States ground water has a pH > 7.5 (DeSimone et al., 2015), and the thermodynamic stage is set for Mn-based catabolisms. It is especially enlightening to note that the inoculum used to demonstrate the first and only example of a microorganism catalyzing the oxidation of Mn^{2+} with O_2 to gain energy was unsterilized municipal drinking water from Pasadena, California, which is typically a mixture of aquifer and surface water sources (Yu and Leadbetter, 2020).

If microorganisms are to gain energy from the manganese reactions considered in this study, they must be able to catalyze these reactions before abiotic processes consume the reactants, even though this is no guarantee that they will reap the energetic rewards. For instance, microorganisms have been shown to oxidize Mn^{2+} up to five orders of magnitude faster than abiotic oxidation (Tebo et al., 2004) and they are thought to dominate Mn^{2+} oxidation in most aquatic settings (Tebo et al., 2004, 2005). Despite the ubiquity of microbial Mn^{2+} oxidation, and the fact that Reaction 5 (O_2 reduction) is exergonic above pH ∼4 (**Figure 4A**), it was only recently shown that a microorganism was able to use the energy liberated by this process (Yu and Leadbetter, 2020). The calculations summarized in **Figures 4B–E** show that it is thermodynamically possible that other electron acceptors are capable of oxidizing Mn^{2+}, particularly NO_2^- and NO_3^-, over a broad range of conditions that can be found in marine settings. In fact, laboratory incubations have demonstrated the oxidation of Mn^{2+} by NO_3^- (forming N_2, Reaction 8) in sediments taken from continental margins (Luther et al., 1997) and Long Island Sound (Hulth et al., 1999), a process that had been previously proposed to occur (Aller et al., 1990; Schulz et al., 1994; Murray et al., 1995). Hulth et al. (1999) report a Gibbs energy for this reaction of −6.11 kJ (mol e$^-$)$^{-1}$ at pH 7 and −8.93 kJ (mol e$^-$)$^{-1}$ at pH 8. By comparison, we determined values of −10.3 kJ (mol e$^-$)$^{-1}$ and −14.9 kJ (mol e$^-$)$^{-1}$ at these values of pH. The differences are due to the differing activities of the aqueous species, particularly the concentration of N_2 used in the reactions quotient, Equation 2: Hulth et al. (1999) used atmospheric N_2 partial pressure (0.781 atm) and we used an activity of 10^{-4}).

A number of studies have reported abiotic manganese disproportionation and comproportionation reactions in laboratory experiments. Typically, these experiments involve exposing an Mn-oxide to Mn^{2+}, and analyzing the resulting material for particular Mn phases. For instance, several authors report that comproportionation reactions, like Reaction 3, are responsible for the formation of MnOOH when Mn^{2+} is added to birnessite (δ-MnO_2) (Tu et al., 1994; Elzinga, 2011; Zhao et al., 2016). Under similar experimental conditions, both Mn disproportionation and comproportionation have been reported (Elzinga and Kustka, 2015; Elzinga, 2016; Hinkle et al., 2016). The addition of complex organic substances to Mn^{2+} and Mn-oxide can lead to the formation of MnOOH and Mn_3O_4 phases (Wang et al., 2018), while the addition of bacterial spore coatings are thought to drive both comproportionation and disproportionation reactions (Bargar et al., 2005). *Bacillus* spores have also been shown to be associated with the formation of mixed (i.e., III/IV) Mn-oxides over a broad range of temperatures (0–80°C) and Mn^{2+} concentrations (<1 nM to >25 mM), using a variety of ionic strengths (1 M HEPES and seawater) (Mandernack et al., 1995). Spore coats from marine *Bacillus* species at pH 7.5 have been shown to oxidize Mn^{2+} to amorphous Mn-oxide that later recrystallized to hausmannite (Mann et al., 1988).

The rates of the comproportionation and disproportionation reactions noted above are difficult to discern because these reactions are typically inferred based on an analysis of the Mn phases at the conclusion of the experiments. However, most of the experiments took place over days or weeks, so microorganisms would likely be able to catalyze the inferred reactions faster than the abiotic reactions occur. This is certainly the case with abiotic Mn^{2+} oxidation, which is kinetically slow (Hinkle et al., 2016 and references therein). On the other side of the catalytic spectrum, Mn^{3+} disproportionates rapidly abiotically, though when it complexes with organics and pyrophosphate, it remains stable

(Kostka et al., 1995; Klewicki and Morgan, 1998; Luther et al., 1999; Parker et al., 2004) for an undetermined amount of time. Mn-oxides have been shown to catalyze the disproportionation of Mn(III)-phosphate complexes at high and low pH (Qian et al., 2019). It should also be noted that bacteriogenic MnO_2, which is riddled with crystallographic defects filled with other cations, is quickly reduced to Mn^{2+} in the presence of ligands or sunlight (Spiro et al., 2010). Furthermore, as the amount of energy available from these redox reactions decreases, the rate of microbial catalysis can drop below detection levels (Jin and Bethke, 2003; LaRowe et al., 2012), perhaps even fading to 0 despite a remaining energetic drive (i.e., $\Delta G_r < 0$) (Schink, 1997; Curtis, 2003; Jin and Bethke, 2003; Hoehler, 2004; LaRowe and Van Cappellen, 2011). Consequently, any search for novel Mn-based metabolisms should be focused on the combinations of temperature and composition that yield the most negative value of ΔG_r: neutral to basic pH for comproportionation reactions as well as Mn^{2+} oxidation by NO_2^-, NO_3^-, and FeOOH; and nearly any conditions for Mn(III) disproportionation.

DATA AVAILABILITY STATEMENT

The original contributions presented in the study are included in the article/**Supplementary Material**, further inquiries can be directed to the corresponding author/s.

AUTHOR CONTRIBUTIONS

DL and JA conceived of the study. DL carried out the calculations and wrote the manuscript with input from JA. HC contributed to the display items and the bibliography. All authors contributed to the article and approved the submitted version.

FUNDING

This work was supported by the NSF-sponsored Center for Dark Energy Biosphere Investigations (C-DEBI) under grant OCE0939564 (JA, DL), the NASA-NSF Origins of Life Ideas Lab program under grant NNN13D466T (DL), and NASA Habitable Worlds program under grant 80NSSC20K0228 (DL). This is C-DEBI contribution 567.

SUPPLEMENTARY MATERIAL

The Supplementary Material for this article can be found online at: https://www.frontiersin.org/articles/10.3389/fmicb.2021.636145/full#supplementary-material

REFERENCES

Akerman, N. H., Price, R. E., Pichler, T., and Amend, J. P. (2011). Energy sources for chemolithotrophs in an arsenic- and iron-rich shallow-sea hydrothermal system. *Geobiology* 9, 436–445. doi: 10.1111/j.1472-4669.2011.00291.x

Akter, T., Jhohura, F. T., Akter, F., Chowdhury, T. R., Mistry, S. K., Dey, D., et al. (2016). Water Quality Index for measuring drinking water quality in rural Bangladesh: a cross-sectional study. *J. Health Population Nutr.* 35:4.

Aller, R. C., Charnock, H., Edmond, J. M., McCave, I. N., Rice, A. L., and Wilson, T. R. S. (1990). Bioturbation and manganese cycling in hemipelagic sediments. *Phil. Trans. R. Soc. Lon. Ser A Math. Phys. Sci.* 331, 51–68. doi: 10.1098/rsta.1990.0056

Amend, J. P., Aronson, H. S., Macalady, J., and LaRowe, D. E. (2020). Another chemolithotrophic metabolism missing in nature: sulfur comproportionation. *Environ. Microbiol.* 22, 1971–1976. doi: 10.1111/1462-2920.14982

Amend, J. P., and LaRowe, D. E. (2019). Minireview: demystifying microbial reaction energetics. *Environ. Microbiol.* 21, 3539–3547. doi: 10.1111/1462-2920.14778

Amend, J. P., LaRowe, D. E., McCollom, T. M., and Shock, E. L. (2013). The energetics of organic synthesis inside and outside the cell. *Phil. Trans. Royal Soc. B* 368, 1–15.

Amend, J. P., McCollom, T. M., Hentscher, M., and Bach, W. (2011). Catabolic and anabolic energy for chemolithoautotrophs in deep-sea hydrothermal systems hosted in different rock types. *Geochim. Cosmochim. Ac.* 75, 5736–5748. doi: 10.1016/j.gca.2011.07.041

Amend, J. P., Rogers, K. L., Shock, E. L., Gurrieri, S., and Inguaggiato, S. (2003). Energetics of chemolithoautotrophy in the hydrothermal system of Vulcano Island, southern Italy. *Geobiology* 1, 37–58. doi: 10.1046/j.1472-4669.2003.00006.x

Bach, W. (2016). Some compositional and kinetic controls on the bioenergetic landscape in oceanic basement. *Front. Microbiol.* 7:107.

Bach, W., and Edwards, K. J. (2003). Iron and sulfide oxidation within the basaltic ocean crust: Implications for chemolithoautotrophic microbial biomass production. *Geochim. Cosmochim. Acta* 67, 3871–3887. doi: 10.1016/s0016-7037(03)00304-1

Bargar, J. R., Tebo, B. M., Bergmann, U., Webb, S. M., Glatzel, P., Chiu, V. Q., et al. (2005). Biotic and abiotic products of Mn(II) oxidation by spores of the marine Bacillus sp. strain SG-1. *Am. Mineral.* 90, 143–154. doi: 10.2138/am.2005.1557

Barnes, R. O., and Goldberg, E. D. (1976). Methane production and consumption in anoxic marine sediments. *Geology* 4, 297–300. doi: 10.1130/0091-7613(1976)4<297:mpacia>2.0.co;2

Berenguer, J. (2011). "Thermophile," in *Encyclopedia of Astrobiology*, eds M. Gargaud, R. Amils, J. C. Quintanilla, H. J. Cleaves, W. M. Irvine, D. L. Pinti, et al. (Berlin: Springer), 1666–1667.

Blöthe, M., Wegorzewski, A., Müller, C., Simon, F., Kuhn, T., and Schippers, A. (2015). Manganese-cycling microbial communities inside deep-sea manganese nodules. *Environ. Sci. Technol.* 49, 7692–7700. doi: 10.1021/es504930v

Boetius, A., Ravenschlag, K., Schubert, C. J., Rickert, D., Widdel, F., Gieseke, A., et al. (2000). A marine microbial consortium apparently mediating anaerobic oxidation of methane. *Nature* 407, 623–626. doi: 10.1038/35036572

Boettger, J., Lin, H. T., Cowen, J. P., Hentscher, M., and Amend, J. P. (2013). Energy yields from chemolithotrophic metabolisms in igneous basement of the Juan de Fuca ridge flank system. *Chem. Geol.* 337, 11–19. doi: 10.1016/j.chemgeo.2012.10.053

Bradley, J. A., Amend, J. P., and LaRowe, D. E. (2018a). Bioenergetic controls on microbial ecophysiology in marine sediments. *Front. Microbiol.* 9:180.

Bradley, J. A., Amend, J. P., and LaRowe, D. E. (2018b). Necromass as a limited source of energy for microorganisms in marine sediments. *J. Geophys. Res. Biogeosci.* 123, 577–590. doi: 10.1002/2017jg004186

Bradley, J. A., Amend, J. P., and LaRowe, D. E. (2019). Survival of the fewest: Microbial dormancy and maintenance in marine sediments through deep time. *Geobiology* 17, 43–59. doi: 10.1111/gbi.12313

Bradley, J. A., Arndt, S., Amend, J. P., Burwicz, E., Dale, A. W., Egger, M., et al. (2020). Widespread energy limitation to life in global subseafloor sediments. *Sci. Adv.* 6:eaba0697. doi: 10.1126/sciadv.aba0697

Bricker, O. (1965). Some stability relations in the system Mn-O2-H2O at 25o and one atmosphere total pressure. *Am. Mineral.* 50, 1296–1354.

Broda, E. (1977). Two kinds of lithotrophs missing in nature. *Zeitschrift Für Allgemeine Mikrobiol.* 17, 491–493. doi: 10.1002/jobm.19770170611

Burdige, D. J. (1993). The biogeochemistry of manganese and iron reduction in marine sediments. *Earth Sci. Rev.* 35, 249–284. doi: 10.1016/0012-8252(93)90040-e

Burdige, D. J., Dhakar, S. P., and Nealson, K. H. (1992). Effects of manganese oxide mineralogy on microbial and chemical manganese reduction. *Geomicrobiol. J.* 10, 27–48. doi: 10.1080/01490459209377902

Burdige, D. J., and Nealson, K. H. (1985). Microbial manganese reduction by enrichment cultures from coastal marine sediments. *Appl. Environ. Microbiol.* 50, 491–497. doi: 10.1128/aem.50.2.491-497.1985

Cardace, D., Meyer-Dombard, D. A. R., Woycheese, K. M., and Arcilla, C. A. (2015). Feasible metabolisms in high pH springs of the Philippines. *Front. Microbiol.* 6:10.

Cerrato, J. M., Falkinham, J. O., Dietrich, A. M., Knocke, W. R., McKinney, C. W., and Pruden, A. (2010). Manganese-oxidizing and -reducing microorganisms isolated from biofilms in chlorinated drinking water systems. *Water Res.* 44, 3935–3945. doi: 10.1016/j.watres.2010.04.037

Chapnick, S. D., Moore, W. S., and Nealson, K. H. (1982). Microbially mediated manganese oxidation in a freshwater lake1. *Limnol. Oceanogr.* 27, 1004–1014. doi: 10.4319/lo.1982.27.6.1004

Chase, M. W. Jr. (1998). *NIST-JANAF Themochemical Tables*, 4 Edn. College Park MD: American Institute of Physics,

Chin, C. S., Coale, K. H., Elrod, V. A., Johnson, K. S., Massoth, G. J., and Baker, E. T. (1994). In situ observations of dissolved iron and manganese in hydrothermal vent plumes. *Juan de Fuca Ridge. J. Geophys. Res. Solid Earth* 99, 4969–4984. doi: 10.1029/93jb02036

Clement, B. G., Luther, G. W., and Tebo, B. M. (2009). Rapid, oxygen-dependent microbial Mn(II) oxidation kinetics at sub-micromolar oxygen concentrations in the Black Sea suboxic zone. *Geochimica et Cosmochimica Acta* 73, 1878–1889. doi: 10.1016/j.gca.2008.12.023

Costa, E., Perez, J., and Kreft, J. U. (2006). Why is metabolic labour divided in nitrification? *Trends Microbiol.* 14, 213–219. doi: 10.1016/j.tim.2006.03.006

Curtis, G. P. (2003). Comparison of approaches for simulating reactive solute transport involving organic degradation reactions by multiple terminal electron acceptors. *Comp. Geosci.* 29, 319–329. doi: 10.1016/s0098-3004(03)00008-6

Dahle, H., Okland, I., Thorseth, I. H., Pederesen, R. B., and Steen, I. H. (2015). Energy landscapes shape microbial communities in hydrothermal systems on the Arctic Mid-Ocean Ridge. *ISME J.* 9, 1593–1606. doi: 10.1038/ismej.2014.247

Daims, H., Lebedeva, E. V., Pjevac, P., Han, P., Herbold, C., Albertsen, M., et al. (2015). Complete nitrification by *Nitrospira* bacteria. *Nature* 528, 504–509. doi: 10.1038/nature16461

Davison, W. (1993). Iron and manganese in lakes. *Earth Sci. Rev.* 34, 119–163. doi: 10.1016/0012-8252(93)90029-7

Daye, M., Klepac-Ceraj, V., Pajusalu, M., Rowland, S., Farrell-Sherman, A., Beukes, N., et al. (2019). Light-driven anaerobic microbial oxidation of manganese. *Nature* 576, 311–314. doi: 10.1038/s41586-019-1804-0

de Lange, G. J., van Os, B., and Poorter, R. (1992). Geochemical composition and inferred accretion rates of sediments and managanese nodules from a submarine hill in the Madeira Abyssal Plain, eastern North Atlantic. *Mar. Geol.* 109, 171–194. doi: 10.1016/0025-3227(92)90227-9

de Meyer, C. M. C., Rodríguez, J. M., Carpio, E. A., García, P. A., Stengel, C., and Berg, M. (2017). Arsenic, manganese and aluminum contamination in groundwater resources of Western Amazonia (Peru). *Sci. Total Environ.* 60, 1437–1450. doi: 10.1016/j.scitotenv.2017.07.059

Dellwig, O., Schnetger, B., Brumsack, H.-J., Grossart, H.-P., and Umlauf, L. (2012). Dissolved reactive manganese at pelagic redoxclines (part II): Hydrodynamic conditions for accumulation. *J. Mar. Syst.* 90, 31–41. doi: 10.1016/j.jmarsys.2011.08.007

DeSimone, L. A., McMahon, P. B., and Rosen, M. R. (2015). *The Quality of Our Nation's Waters: Water Quality in Principal Aquifers of the United States, 1991-2010, Circular*. Reston, VA: U.S. Geological Survey, 161.

Dick, J. M. (2019). CHNOSZ: thermodynamic calculations and diagrams for geochemistry. *Front. Earth Sci.* 7:180.

Duckworth, O. W., and Sposito, G. (2005). Siderophore-Manganese(III) Interactions. I. Air-Oxidation of Manganese(II) Promoted by Desferrioxamine B. *Environ. Sci. Technol.* 39, 6037–6044. doi: 10.1021/es050275k

Edwards, K. J., Bach, W., and McCollom, T. M. (2005). Geomicrobiology in oceanography: microbe–mineral interactions at and below the seafloor. *Trends Microbiol.* 13, 449–456. doi: 10.1016/j.tim.2005.07.005

Eecke, H. C. V., Akerman, N. H., Huber, J. A., Butterfield, D. A., and Holden, J. F. (2013). Growth kinetics and energetics of a deep-sea hyperthermophilic methanogen under varying environmental conditions. *Env. Microbiol. Rep.* 5, 665–671.

Elzinga, E. J. (2011). Reductive Transformation of Birnessite by Aqueous Mn(II). *Environ. Sci. Technol.* 45, 6366–6372. doi: 10.1021/es2013038

Elzinga, E. J. (2016). 54Mn Radiotracers Demonstrate Continuous Dissolution and Reprecipitation of Vernadite (δ-MnO2) during Interaction with Aqueous Mn(II). *Environ. Sci. Technol.* 50, 8670–8677. doi: 10.1021/acs.est.6b02874

Elzinga, E. J., and Kustka, A. B. (2015). A Mn-54 Radiotracer Study of Mn Isotope Solid–Liquid Exchange during Reductive Transformation of Vernadite (δ-MnO2) by Aqueous Mn(II). *Environ. Sci. Technol.* 49, 4310–4316. doi: 10.1021/acs.est.5b00022

Fredrickson, J. K., Zachara, J. M., Kennedy, D. W., Liu, C., Duff, M. C., Hunter, D. B., et al. (2002). Influence of Mn oxides on the reduction of uranium(VI) by the metal-reducing bacterium Shewanella putrefaciens. *Geochimica et Cosmochimica Acta* 66, 3247–3262. doi: 10.1016/s0016-7037(02)00928-6

Froelich, P. N., Klinkhammer, G. P., Bender, M. L., Luedtke, N. A., Heath, G. R., Cullen, D., et al. (1979). Early oxidation of organic matter in pelagic sediments of the eastern equatorial Atlantic: suboxic diagenesis. *Geochim. Cosmochim. Acta* 43, 1075–1090. doi: 10.1016/0016-7037(79)90095-4

Gao, Y., Leermakers, M., Elskens, M., Billon, G., Ouddane, B., Fischer, J. C., et al. (2007). High resolution profiles of thallium, manganese and iron assessed by DET and DGT techniques in riverine sediment pore waters. *Sci. Total Environ.* 373, 526–533. doi: 10.1016/j.scitotenv.2006.11.047

Gounot, A.-M. (1994). Microbial oxidation and reduction of manganese: Consequences in groundwater and applications. *FEMS Microbiol. Rev.* 14, 339–349. doi: 10.1111/j.1574-6976.1994.tb00108.x

Hamer, K., Gudenschwager, I., and Pichler, T. (2020). Manganese (Mn) concentrations and the mn-fe relationship in shallow groundwater: implications for groundwater monitoring. *Soil Syst.* 4, 1–19.

Han, Y., and Perner, M. (2015). The globally widespread genus Sulfurimonas: versatile energy metabolisms and adaptations to redox clines. *Front. Microbiol.* 6:989.

Hansel, C. M. (2017). "Chapter two - manganese in marine microbiology," in *Advances in Microbial Physiology*, ed. R. K. Poole (Cambridge MA: Academic Press), 37–83. doi: 10.1016/bs.ampbs.2017.01.005

Hein, J. R. (2013). "Manganese Nodules," in *Encyclopedia of Marine Geosciences*, eds J. Harff, M. Meschede, S. Petersen, and J. Thiede (Dordrecht: Springer), 1–7.

Heintze, S. G., and Mann, P. J. G. (1947). Soluble complexes of manganic manganese. . *Agric. Sci.* 37, 23–26. doi: 10.1017/s0021859600013009

Helgeson, H. C. (1969). Thermodynamics of hydrothermal systems at elevated temperatures and pressures. *Amer. J. Sci.* 267, 729–804. doi: 10.2475/ajs.267.7.729

Helgeson, H. C., Delany, J. M., Nesbitt, H. W., and Bird, D. K. (1978). Summary and critique of the thermodynamic properties of rock-forming minerals. *Amer. J. Sci.* 278, 1–229.

Helgeson, H. C., Kirkham, D. H., and Flowers, G. C. (1981). Theoretical prediction of thermodynamic behavior of aqueous electrolytes at high pressures and temperatures: 4. Calculation of activity coefficients, osmotic coefficients, and apparent molal and standard and relative partial molal properties to 600oC and 5 kb. *Amer. J. Sci.* 281, 1249–1516. doi: 10.2475/ajs.281.10.1249

Hem, J. D., Roberson, C. E., and Fournier, R. B. (1982). Stability of βMnOOH and manganese oxide deposition from springwater. *Water Resour. Res.* 18, 563–570. doi: 10.1029/wr018i003p00563

Henkel, J. V., Dellwig, O., Pollehne, F., Herlemann, D. P. R., Leipe, T., and Schulz-Vogt, H. N. (2019). A bacterial isolate from the Black Sea oxidizes sulfide with manganese(IV) oxide. *Proc. Natl. Acad. Sci.U.S.A.* 116, 12153–12155. doi: 10.1073/pnas.1906000116

Hentscher, M., and Bach, W. (2012). Geochemically induced shifts in catabolic energy yields explain past ecological changes of diffuse vents in the East Pacific Rise 9° 50′N area. *Geochem. T.* 13:2.

Hinkle, M. A. G., Flynn, E. D., and Catalano, J. G. (2016). Structural response of phyllomanganates to wet aging and aqueous Mn(II). *Geochimica et Cosmochimica Acta* 192, 220–234. doi: 10.1016/j.gca.2016.07.035

Hinrichs, K.-U., Hayes, J. M., Sylva, S. P., Brewer, P. G., and DeLong, E. F. (1999). Methane-consuming archaebacteria in marine sediments. *Nature* 398, 802–805. doi: 10.1038/19751

Hoehler, T. M. (2004). Biological energy requirements as quantitative boundary conditions for life in the subsurface. *Geobiology* 2, 205–215. doi: 10.1111/j.1472-4677.2004.00033.x

Homoncik, S. C., MacDonald, A. M., Heal, K. V., Ó Dochartaigh, B. É, and Ngwenya, B. T. (2010). Manganese concentrations in Scottish groundwater. *Sci. Total Environ.* 408, 2467–2473. doi: 10.1016/j.scitotenv.2010.02.017

Hou, Q., Zhang, Q., Huang, G., Liu, C., and Zhang, Y. (2020). Elevated manganese concentrations in shallow groundwater of various aquifers in a rapidly urbanized delta, south China. *Sci. Total Environ.* 701:134777. doi: 10.1016/j.scitotenv.2019.134777

Hulth, S., Aller, R. C., and Gilbert, F. (1999). Coupled anoxic nitrification/manganese reduction in marine sediments. *Geochimica et Cosmochimica Acta* 63, 49–66. doi: 10.1016/s0016-7037(98)00285-3

Inskeep, W. P., Ackerman, G. G., Taylor, W. P., Kozubal, M., Korf, S., and Macur, R. E. (2005). On the energetics of chemolithotrophy in nonequilibrium systems: case studies of geothermal springs in Yellowstone National Park. *Geobiology* 3, 297–317. doi: 10.1111/j.1472-4669.2006.00059.x

Jiang, X.-D., Sun, X.-M., and Guan, Y. (2019). Biogenic mineralization in the ferromanganese nodules and crusts from the South China Sea. *J. Asian Earth Sci.* 171, 46–59. doi: 10.1016/j.jseaes.2017.07.050

Jin, Q., and Bethke, C. M. (2003). A new rate law describing microbial respiration. *Appl. Environ. Microbiol.* 69, 2340–2348. doi: 10.1128/aem.69.4.2340-2348.2003

Johnson, J. E., Savalia, P., Davis, R., Kocar, B. D., Webb, S. M., Nealson, K. H., et al. (2016). Real-time manganese phase dynamics during biological and abiotic manganese oxide reduction. *Environ. Sci. Technol.* 50, 4248–4258. doi: 10.1021/acs.est.5b04834

Johnson, J. W., Oelkers, E. H., and Helgeson, H. C. (1992). SUPCRT92 - A software package for calculating the standard molal thermodynamic properties of minerals, gases, aqueous species, and reactions from 1 bar to 5000 bar and 0oC to 1000oC. *Comput. Geosci.* 18, 899–947. doi: 10.1016/0098-3004(92)90029-q

Jones, M. R., Luther, G. W., and Tebo, B. M. (2020). Distribution and concentration of soluble manganese(II), soluble reactive Mn(III)-L, and particulate MnO2 in the Northwest Atlantic Ocean. *Mar. Chem.* 226:103858. doi: 10.1016/j.marchem.2020.103858

Kasten, S., Freudenthal, T., Gingele, F. X., and Schulz, H. D. (1998). Simultaneous formation of iron-rich layers at different redox boundaries in sediments of the Amazon deep-sea fan. *Geochimica et Cosmochimica Acta* 62, 2253–2264. doi: 10.1016/s0016-7037(98)00093-3

Kato, S., Hirai, M., Ohkuma, M., and Suzuki, K. (2019). Microbial metabolisms in an abyssal ferromanganese crust from the Takuyo-Daigo Seamount as revealed by metagenomics. *PLoS One* 14:e0224888. doi: 10.1371/journal.pone.0224888

Kiel Reese, B., Zinke, L. A., Sobol, M. S., LaRowe, D. E., Orcutt, B. N., Zhang, X., et al. (2018). Nitrogen cycling of active bacteria within oligotrophic sediment of the Mid-Atlantic Ridge Flank. *Geomicrobiol. J.* 35, 1–16. doi: 10.1080/01490451.01492017.01392649

Klewicki, J. K., and Morgan, J. J. (1998). Kinetic Behavior of Mn(III) Complexes of Pyrophosphate, EDTA, and Citrate. *Environ. Sci. Technol.* 32, 2916–2922. doi: 10.1021/es980308e

Klinkhammer, G., Bender, M. and Weiss, R. F. (1977). Hydrothermal manganese in the Galapagos Rift. *Nature* 269, 319–320.

Knittel, K., Wegener, G., and Boetius, A. (2019). "Anaerobic methane oxidizers," in *Microbial Communities Utilizing Hydrocarbons and Lipids: Members, Metagenomics and Ecophysiology*, ed. T. J. McGenity (Cham: Springer International Publishing), 113–132. doi: 10.1007/978-3-030-14785-3_7

Kostka, J. E., Luther, G. W., and Nealson, K. H. (1995). Chemical and biological reduction of Mn (III)-pyrophosphate complexes: potential importance of dissolved Mn (III) as an environmental oxidant. *Geochimica et Cosmochimica Acta* 59, 885–894. doi: 10.1016/00167-0379(50)00070-

Kuypers, M. M. M., Sliekers, A. O., Lavik, G., Schmid, M., Jørgensen, B. B., Kuenen, J. G., et al. (2003). Anaerobic ammonium oxidation by anammox bacteria in the Black Sea. *Nature* 422, 608–611. doi: 10.1038/nature01472

LaRowe, D. E., and Amend, J. P. (2014). "Energetic constraints on life in marine deep sediments," in *Life in Extreme Environments: Microbial Life in the Deep Biosphere*, eds J. Kallmeyer and K. Wagner (Berlin: de Gruyter), 279–302.

LaRowe, D. E., and Amend, J. P. (2015a). Catabolic rates, population sizes and doubling/replacement times of microorganisms in the natural settings. *Am. J. Sci.* 315, 167–203. doi: 10.2475/03.2015.01

LaRowe, D. E., and Amend, J. P. (2015b). Power limits for microbial life. *Front. Extr. Microbiol.* 6:718.

LaRowe, D. E., and Amend, J. P. (2016). The energetics of anabolism in natural settings. *ISME J.* 10, 1285–1295. doi: 10.1038/ismej.2015.227

LaRowe, D. E., and Amend, J. P. (2019). The energetics of fermentation in natural settings. *Geomicrobiol. J.* 36, 492–505. doi: 10.1080/01490451.2019.1573278

LaRowe, D. E., and Amend, J. P. (2020). "Energy limits for life in the subsurface," in *Whole Earth Carbon: Past to Present*, eds B. N. Orcutt, I. Daniel, and R. Dasgupta (Cambridge: Cambridge University Press), 585–619. doi: 10.1017/9781108677950.019

LaRowe, D. E., Dale, A. W., Aguilera, D. R., L'Heureux, I., Amend, J. P., and Regnier, P. (2014). Modeling microbial reaction rates in a submarine hydrothermal vent chimney wall Geochim. *Cosmochim. Acta* 124, 72–97. doi: 10.1016/j.gca.2013.09.005

LaRowe, D. E., Dale, A. W., Amend, J. P., and Van Cappellen, P. (2012). Thermodynamic limitations on microbially catalyzed reaction rates. *Geochim. Cosmochim. Acta* 90, 96–109. doi: 10.1016/j.gca.2012.05.011

LaRowe, D. E., and Regnier, P. (2008). Thermodynamic potential for the abiotic synthesis of adenine, cytosine, guanine, thymine, uracil, ribose and deoxyribose in hydrothermal systems. *Orig. Life Evol. Bios.* 38, 383–397. doi: 10.1007/s11084-008-9137-2

LaRowe, D. E., and Van Cappellen, P. (2011). Degradation of natural organic matter: A thermodynamic analysis. *Geochim. Cosmochim. Acta* 75, 2030–2042. doi: 10.1016/j.gca.2011.01.020

Larsen, I., Little, B., Nealson, K. H., Ray, R., Stone, A., and Tian, J. (1998). Manganite reduction by Shewanella putrefaciens MR-4. *Am. Mineral.* 83, 1564–1572. doi: 10.2138/am-1998-11-1244

Lovley, D. R., and Phillips, E. J. P. (1988). Novel mode of microbial energy metabolism: organic carbon oxidation coupled to dissimilatory reduction of iron or manganese. *Appl. Environ. Microbiol.* 54:1472. doi: 10.1128/aem.54.6.1472-1480.1988

Lu, G.-S., LaRowe, D. E., Gilhooly, W. P. III, Druschel, G. K., Fike, D. A., Price, R. E., et al. (2020). Bioenergetic characterization of a shallow-sea hydrothermal vent system: Milos Island. Greece. *PLoS One* 15:e0234175. doi: 10.1371/journal.pone.0234175

Luther, G. W., Ruppel, D. T., and Burkhard, C. (1999). *Reactivity of Dissolved Mn(III) Complexes and Mn(IV) Species with Reductants: Mn Redox Chemistry Without a Dissolution Step?, Mineral-Water Interfacial Reactions*. Washington DC: American Chemical Society, 265–280.

Luther, G. W., Sundby, B., Lewis, B. L., Brendel, P. J., and Silverberg, N. (1997). Interactions of manganese with the nitrogen cycle: alternative pathways to dinitrogen. *Geochimica et Cosmochimica Acta* 61, 4043–4052. doi: 10.1016/s0016-7037(97)00239-1

Madison, A. S., Tebo, B. M., and Luther, G. W. (2011). Simultaneous determination of soluble manganese(III), manganese(II) and total manganese in natural (pore)waters. *Talanta* 84, 374–381. doi: 10.1016/j.talanta.2011.01.025

Madison, A. S., Tebo, B. M., Mucci, A., Sundby, B., and Luther, G. W. (2013). Abundant Porewater Mn(III) Is a Major Component of the Sedimentary Redox System. *Science* 341, 875. doi: 10.1126/science.1241396

Maier, C. G., and Kelley, K. K. (1932). An equation for the representation of high-temperature heat content data. *J. Amer. Chem. Soc.* 54, 3243–3246. doi: 10.1021/ja01347a029

Mandernack, K. W., Post, J., and Tebo, B. M. (1995). Manganese mineral formation by bacterial spores of the marine Bacillus, strain SG-1: Evidence for the direct oxidation of Mn(II) to Mn(IV). *Geochimica et Cosmochimica Acta* 59, 4393–4408. doi: 10.1016/0016-7037(95)00298-e

Mann, S., Sparks, N. H., Scott, G. H., and de Vrind-de Jong, E. W. (1988). Oxidation of Manganese and Formation of Mn(3)O(4) (Hausmannite) by Spore Coats of a Marine *Bacillus* sp. *Appl. Environ. Microbiol.* 54, 2140–2143. doi: 10.1128/aem.54.8.2140-2143.1988

März, C., Hoffmann, J., Bleil, U., de Lange, G. J., and Kasten, S. (2008). Diagenetic changes of magnetic and geochemical signals by anaerobic methane oxidation in sediments of the Zambezi deep-sea fan (SW Indian Ocean). *Mar. Geol.* 255, 118–130. doi: 10.1016/j.margeo.2008.05.013

McCollom, T. M. (2000). Geochemical constraints on primary productivity in submarine hydrothermal vent plumes. *Deep Sea Res. Part I Oceanogr. Res. Pap.* 47, 85–101. doi: 10.1016/s0967-0637(99)00048-5

McCollom, T. M. (2007). Geochemical constraints on sources of metabolic energy for chemolithoautotrophy in ultramafic-hosted deep-sea hydrothermal systems. *Astrobiology* 7, 933–950. doi: 10.1089/ast.2006.0119

McCollom, T. M., and Amend, J. P. (2005). A thermodynamic assessment of energy requirements for biomass synthesis by chemolithoautotrophic microorganisms in oxic and anoxic environments. *Geobiology* 3, 135–144. doi: 10.1111/j.1472-4669.2005.00045.x

McCollom, T. M., and Shock, E. L. (1997). Geochemical constraints on chemolithoautotrophic metabolism by microorganisms in seafloor hydrothermal systems. *Geochim. Cosmochim. Ac.* 61, 4375–4391. doi: 10.1016/s0016-7037(97)00241-x

McKay, L., Klokman, V. W., Mendlovitz, H. P., LaRowe, D. E., Hoer, D. R., Albert, D., et al. (2016). Thermal and geochemical influences on microbial biogeography in the hydrothermal sediments of Guaymas Basin. *Gulf California. Env. Microbiol. Rep.* 8, 150–161. doi: 10.1111/1758-2229.12365

McMahon, P. B., Belitz, K., Reddy, J. E., and Johnson, T. D. (2019). Elevated manganese concentrations in united states groundwater, role of land surface–soil–aquifer connections. *Environ. Sci. Technol.* 53, 29–38. doi: 10.1021/acs.est.8b04055

McQuay, E. L., Torres, M. E., Collier, R. W., Huh, C.-A., and McManus, J. (2008). Contribution of cold seep barite to the barium geochemical budget of a marginal basin. *Deep Sea Res. Part I Oceanogr. Res. Pap.* 55, 801–811. doi: 10.1016/j.dsr.2008.03.001

Murray, J. W., Codispoti, L. A., and Friederich, G. E. (1995). "Oxidation-reduction environments: The suboxic zone of the Black Sea," in *Aquatic Chemistry: Interfacial and Interspecies Processes*, ed. C. P. E. A. Huang (Washington DC: American Chemical Society), 157–176. doi: 10.1021/ba-1995-0244.ch007

Myers, C. R., and Nealson, K. H. (1988). Bacterial manganese reduction and growth with manganese oxide as the sole electron acceptor. *Science* 240:1319. doi: 10.1126/science.240.4857.1319

Nealson, K. H., Tebo, B. M., and Rosson, R. A. (1988). "Occurrence and Mechanisms of Microbial Oxidation of Manganese," in *Advances in Applied Microbiology*, ed. A. I. Laskin (Cambridge MA: Academic Press), 279–318. doi: 10.1016/s0065-2164(08)70209-0

Northup, D. E., Barns, S. M., Yu, L. E., Spilde, M. N., Schelble, R. T., Dano, K. E., et al. (2003). Diverse microbial communities inhabiting ferromanganese deposits in Lechuguilla and Spider Caves. *Environ. Microbiol.* 5, 1071–1086. doi: 10.1046/j.1462-2920.2003.00500.x

Oldham, V. E., Jones, M. R., Tebo, B. M., and Luther, G. W. (2017a). Oxidative and reductive processes contributing to manganese cycling at oxic-anoxic interfaces. *Mar. Chem.* 195, 122–128. doi: 10.1016/j.marchem.2017.06.002

Oldham, V. E., Mucci, A., Tebo, B. M., and Luther, G. W. (2017b). Soluble Mn(III)–L complexes are abundant in oxygenated waters and stabilized by humic ligands. *Geochimica et Cosmochimica Acta* 199, 238–246. doi: 10.1016/j.gca.2016.11.043

Oldham, V. E., Owings, S. M., Jones, M. R., Tebo, B. M., and Luther, G. W. (2015). Evidence for the presence of strong Mn(III)-binding ligands in the water column of the Chesapeake Bay. *Mar. Chem.* 171, 58–66. doi: 10.1016/j.marchem.2015.02.008

Orcutt, B. N., Bradley, J. A., Brazelton, W. J., Estes, E. R., Goordial, J. M., Huber, J. A., et al. (2020). Impacts of deep-sea mining on microbial ecosystem services. *Limnol. Oceanogr.* 65, 1489–1510. doi: 10.1002/lno.11403

Orphan, V. J., House, C. H., Hinrichs, K.-U., McKeegan, K. D., and DeLong, E. F. (2001). Methane-consuming archaea revealed by directly coupled isotopic and phylogenetic analysis. *Science* 293, 484–487. doi: 10.1126/science.1061338

Osburn, M. R., LaRowe, D. E., Momper, L., and Amend, J. P. (2014). Chemolithotrophy in the continental deep subsurface: Sanford Underground Research Facility (SURF), USA. *Front. Extr. Microbiol.* 5:610.

Parker, D. L., Sposito, G., and Tebo, B. M. (2004). Manganese(III) binding to a pyoverdine siderophore produced by a manganese(II)-oxidizing bacterium. *Geochimica et Cosmochimica Acta* 68, 4809–4820. doi: 10.1016/j.gca.2004.05.038

Price, R. E., LaRowe, D. E., Italiano, F., Savov, I., Pichler, T., and Amend, J. P. (2015). Subsurface hydrothermal processes and the bioenergetics of chemolithoautotrophy at the shallow-sea vents off Panarea Island (Italy). *Chem. Geol.* 407, 21–45. doi: 10.1016/j.chemgeo.2015.04.011

Qian, A., Zhang, W., Shi, C., Pan, C., Giammar, D. E., Yuan, S., et al. (2019). Geochemical Stability of Dissolved Mn(III) in the Presence of Pyrophosphate as a Model Ligand: Complexation and Disproportionation. *Environ. Sci. Technol.* 53, 5768–5777. doi: 10.1021/acs.est.9b00498

Reed, D. C., Breier, J. A., Jiang, H., Anantharaman, K., Klausmeier, C. A., Toner, B. M., et al. (2015). Predicting the response of the deep-ocean microbiome to geochemical perturbation by hydrothermal vents. *ISME J.* 9, 1857–1869. doi: 10.1038/ismej.2015.4

Robie, R. A., and Bethke, P. M. (1963). *Molar Volumes and Densities of Minerals, Open-File Report Series number 63-114*. Washington D.C: Geological Survey.

Robie, R. A., and Hemingway, B. S. (1985). Low-temperature molar heat capacities and entropies of MnO2 (pyrolusite), Mn3O4 (hausmanite) and Mn2O3 (bixbyite). *J. Chem. Thermodyn.* 17, 165–181. doi: 10.1016/0021-9614(85)90069-2

Rogers, K. L., and Amend, J. P. (2005). Archaeal diversity and geochemical energy yields in a geothermal well on Vulcano Island. *Italy. Geobiology* 3, 319–332. doi: 10.1111/j.1472-4669.2006.00064.x

Rogers, K. L., and Amend, J. P. (2006). Energetics of potential heterotrophic metabolisms in the marine hydrothermal system of Vulcano Island. *Italy. Geochim. Cosmochim. Ac.* 70, 6180–6200. doi: 10.1016/j.gca.2006.08.046

Schaller, T., and Wehrli, B. (1996). Geochemical-focusing of manganese in lake sediments — An indicator of deep-water oxygen conditions. *Aquat. Geochem.* 2, 359–378. doi: 10.1007/bf00115977

Schink, B. (1997). Energetics of synthrophic cooperation in methanogenic degradation. *Microbiol. Mol. Biol. Rev.* 61, 262–280. doi: 10.1128/.61.2.262-280.1997

Schrum, H. N., Spivack, A. J., Kastner, M., and D'Hondt, S. (2009). Sulfate-reducing ammonium oxidation: a thermodynamically feasible metabolic pathway in subseafloor sediment. *Geology* 37, 939–942. doi: 10.1130/g30238a.1

Schulte, M. D., Shock, E. L., and Wood, R. (2001). The temperature dependence of the standard-state thermodynamic properties of aqueous nonelectrolytes. *Geochim. Cosmochim. Acta* 65, 3919–3930. doi: 10.1016/s0016-7037(01)00717-7

Schulz, H. D., Dahmke, A., Schinzel, U., Wallmann, K., and Zabel, M. (1994). Early diagenetic processes, fluxes, and reaction rates in sediments of the South Atlantic. *Geochimica et Cosmochimica Acta* 58, 2041–2060. doi: 10.1016/0016-7037(94)90284-4

Schulz, H. D., and Zabel, M. (2006). *Marine Geochemistry*, 2nd Edn. Berlin: Springer.

Senoh, H., Ueda, M., Furukawa, N., Inoue, H., and Iwakura, C. (1998). Theoretical evaluation for thermodynamic stability of constituents of Mm-based hydrogen storage alloy in 6 M KOH solution at relatively high temperatures. *J. All. Comp.* 280, 114–124. doi: 10.1016/s0925-8388(98)00739-7

Shibuya, T., Russell, M. J., and Takai, K. (2016). Free energy distribution and hydrothermal mineral precipitation in Hadean submarine alkaline vent systems: importance of iron redox reactions under anoxic conditions. *Geochim. Cosmochim. Ac.* 175, 1–19. doi: 10.1016/j.gca.2015.11.021

Shock, E. L., and Helgeson, H. C. (1988). Calculation of the thermodynamic and transport properties of aqueous species at high pressures and temperatures - Correlation algorithms for ionic species and equation of state predictions to 5 kb and 1000oC. *Geochim. Cosmochim. Acta* 52, 2009–2036. doi: 10.1016/0016-7037(88)90181-0

Shock, E. L., Holland, M., Meyer-Dombard, D., and Amend, J. P. (2005). Geochemical sources of energy for microbial metabolism in hydrothermal ecosystems: Obsidian Pool, Yellowstone National Park. *Geother. Biol. Geochem. Yellowstone Natl. Park* 1, 95–112.

Shock, E. L., Holland, M., Meyer-Dombard, D., Amend, J. P., Osburn, G. R., and Fischer, T. P. (2010). Quantifying inorganic sources of geochemical energy in hydrothermal ecosystems, Yellowstone National Park, USA. *Geochim. Cosmochim. Ac.* 74, 4005–4043. doi: 10.1016/j.gca.2009.08.036

Shock, E. L., and Holland, M. E. (2004). "Geochemical energy sources that support the subseafloor biosphere. the subseafloor biosphere at mid-ocean ridges," in *Geophysical Monograph 144*, eds W. S. D. Wilcock, E. F. DeLong, D. S. Kelley, J. A. Baross, and S. C. Cary (Washington D.C: American Geophysical Union), 153–165. doi: 10.1029/144gm10

Shock, E. L., McCollom, T. M., and Schulte, M. D. (1995). Geochemical constraints on chemolithoautotrophic reactions in hydrothermal systems. *Orig. Life Evol. Bios.* 25, 141–159. doi: 10.1007/bf01581579

Shock, E. L., Oelkers, E., Johnson, J., Sverjensky, D., and Helgeson, H. C. (1992). Calculation of the thermodynamic properties of aqueous species at high pressures and temperatures - Effective electrostatic radii, dissociation constants and standard partial molal properties to 1000oC and 5 kbar. *J. Chem. Soc. Faraday Trans.* 88, 803–826. doi: 10.1039/ft9928800803

Shock, E. L., Sassani, D., Willis, M., and Sverjensky, D. (1997). Inorganic species in geologic fluids: correlations among standard molal thermodynamic properties of aqueous ions and hydroxide complexes. *Geochim. Cosmochim. Acta* 61, 907–950. doi: 10.1016/s0016-7037(96)00339-0

Snow, C. L., Lilova, K. I., Radha, A. V., Shi, Q., Smith, S., Navrotsky, A., et al. (2013). Heat capacity and thermodynamics of a synthetic two-line ferrihydrite. *FeOOH*0.027H2O. J. Chem. Thermo.* 58, 307–314. doi: 10.1016/j.jct.2012.11.012

Spear, J. R., Walker, J. J., McCollom, T. M., and Pace, N. R. (2005a). Hydrogen and bioenergetics in the Yellowstone geothermal ecosystem. *PNAS* 102, 2555–2560. doi: 10.1073/pnas.0409574102

Spear, J. R., Walker, J. J., and Pace, N. R. (2005b). "Hydrogen and primary productivity: inference of biogeochemistry from phylogeny in a geothermal ecosystem," in *Geothermal Biology and Geochemistry in Yellowstone National Park*, 1st Edn, eds W. P. Inskeep and T. R. McDermott (Bozeman, MT: Montana State University Publications), 113–128.

Spiro, T. G., Bargar, J. R., Sposito, G., and Tebo, B. M. (2010). Bacteriogenic manganese oxides. *Acc. Chem. Res.* 43, 2–9. doi: 10.1021/ar800232a

Sylvan, J. B., Wankel, S. D., LaRowe, D. E., Charoenpong, C. N., Huber, H., Moyer, C. L., et al. (2017). Evidence for micorbial mediation of subseafloor nitrogen redox processes at Loihi Seamount. *Hawaii. Geochimica et Cosmochimica Acta* 198, 131–150. doi: 10.1016/j.gca.2016.10.029

Szeinbaum, N., Burns, J. L., and DiChristina, T. J. (2014). Electron transport and protein secretion pathways involved in Mn(III) reduction by *Shewanella oneidensis*. *Environ. Microbiol. Rep.* 6, 490–500. doi: 10.1111/1758-2229.12173

Szeinbaum, N., Lin, H., Brandes, J. A., Taillefert, M., Glass, J. B., and DiChristina, T. J. (2017). Microbial manganese(III) reduction fuelled by anaerobic acetate oxidation. *Environ. Microbiol.* 19, 3475–3486. doi: 10.1111/1462-2920.13829

Szeinbaum, N., Nunn, B. L., Cavazos, A. R., Crowe, S. A., Stewart, F. J., DiChristina, T. J., et al. (2020). Novel insights into the taxonomic diversity and molecular mechanisms of bacterial Mn(III) reduction. *Environ. Microbiol. Rep.* 12, 583–593. doi: 10.1111/1758-2229.12867

Tanger, J. C., and Helgeson, H. C. (1988). Calculation of the thermodynamic and transport properties of aqueous species at high pressures and temperatures - Revised equations of state for the standard partial molal properties of ions and electrolytes. *Amer. J. Sci.* 288, 19–98. doi: 10.2475/ajs.288.1.19

Tazaki, K. (2000). Formation of Banded Iron-Manganese Structures by Natural Microbial Communities. *Clays and Clay Minerals* 48, 511–520. doi: 10.1346/ccmn.2000.0480503

Tebo, B. M., Bargar, J. R., Clement, B. G., Dick, G. J., Murray, K. J., Parker, D., et al. (2004). BIOGENIC MANGANESE OXIDES: Properties and Mechanisms of Formation. *Annu. Rev. Earth Planet. Sci.* 32, 287–328. doi: 10.1146/annurev.earth.32.101802.120213

Tebo, B. M., Johnson, H. A., McCarthy, J. K., and Templeton, A. S. (2005). Geomicrobiology of manganese(II) oxidation. *Trends Microbiol.* 13, 421–428. doi: 10.1016/j.tim.2005.07.009

Tebo, B. M., Rosson, R. A., and Nealson, K. H. (1991). "Potential for Manganese(II) Oxidation and Manganese(IV) Reduction to Co-Occur in the Suboxic Zone of the Black Sea," in *Black Sea Oceanography*, eds E. Izdar and J. W. Murray (Dordrecht: Springer), 173–185. doi: 10.1007/978-94-011-2608-3_10

Teske, A., Callaghan, A. V., and LaRowe, D. E. (2014). Biosphere frontiers: Deep life in the sedimented hydrothermal system of Guaymas Basin. *Front. Extr. Microbiol.* 5:362.

Trouwborst, R. E., Clement, B. G., Tebo, B. M., Glazer, B. T., and Luther, G. W. (2006). Soluble Mn(III) in Suboxic Zones. *Science* 313:1955. doi: 10.1126/science.1132876

Tu, S., Racz, G. J., and Goh, T. B. (1994). Transformations of synthetic birnessite as affected by ph and manganese concentration. *Clays Clay Miner.* 42, 321–330. doi: 10.1346/ccmn.1994.0420310

Tully, B., and Heidelberg, J. (2013). Microbial communities associated with ferromanganese nodules and the surrounding sediments. *Front. Microbiol.* 4:161.

van de Graaf, A. A., Mulder, A., de Bruijn, P., Jetten, M. S., Robertson, L. A., and Kuenen, J. G. (1995). Anaerobic oxidation of ammonium is a biologically mediated process. *Appl. Environ. Microbiol.* 61:1246. doi: 10.1128/aem.61.4.1246-1251.1995

van Hulten, M. M. P., Middag, R., Dutay, J.-C., de Baar, H. J. W., Roy-Barman, M., Gehlen, M., et al. (2017). Model output of manganese concentrations from a global ocean circulation model, link to files in NetCDF format, Supplement to: van Hulten, MMP et al. (2017): Manganese in the west Atlantic Ocean in the context of the first global ocean circulation model of manganese. *Biogeosciences* 14, 1123–1152. doi: 10.5194/bg-14-1123-2017

van Kessel, M. A. H. J., Speth, D. R., Albertsen, M., Nielsen, P. H., Op den Camp, H. J. M., Kartal, B., et al. (2015). Complete nitrification by a single microorganism. *Nature* 528, 555–559. doi: 10.1038/nature16459

Vick, T. J., Dodsworth, J. A., Costa, K. C., Shock, E. L., and Hedlund, B. P. (2010). Microbiology and geochemistry of Little Hot Creek, a hot spring environment in the Long Valley Caldera. *Geobiology* 8, 140–154. doi: 10.1111/j.1472-4669.2009.00228.x

Villalobos, M., Toner, B., Bargar, J., and Sposito, G. (2003). Characterization of the manganese oxide produced by *pseudomonas* putida strain MnB1. *Geochimica et Cosmochimica Acta* 67, 2649–2662. doi: 10.1016/s0016-7037(03)00217-5

Wang, G., Spivack, A. J., and D'Hondt, S. (2010). Gibbs energies of reaction and microbial mutualism in anaerobic deep subseafloor sediments of ODP Site 1226. *Geochim. Cosmochim. Acta* 74, 3938–3947. doi: 10.1016/j.gca.2010.03.034

Wang, Q., Yang, P., and Zhu, M. (2018). Structural transformation of birnessite by fulvic acid under anoxic conditions. *Environ. Sci. Technol.* 52, 1844–1853. doi: 10.1021/acs.est.7b04379

Wasserman, G. A., Liu, X., Parvez, F., Ahsan, H., Levy, D., Factor-Litvak, P., et al. (2006). Water manganese exposure and children's intellectual function in Araihazar, Bangladesh. *Environ. Health Perspect.* 114, 124–129. doi: 10.1289/ehp.8030

Windman, T., Zolotova, N., Schwandner, F., and Shock, E. L. (2007). Formate as an energy source for microbial metabolism in chemosynthetic zones of hydrothermal ecosystems. *Astrobiology* 7, 873–890. doi: 10.1089/ast.2007.0127

Wright, M. H., Geszvain, K., Oldham, V. E., Luther, G. W., and Tebo, B. M. (2018). Oxidative Formation and Removal of Complexed Mn(III) by *Pseudomonas* Species. *Frontiers in Microbiology* 9:560.

Yakushev, E., Pakhomova, S., Sørenson, K., and Skei, J. (2009). Importance of the different manganese species in the formation of water column redox zones: Observations and modeling. *Mar. Chem.* 117, 59–70. doi: 10.1016/j.marchem.2009.09.007

Yakushev, E. V., Pollehne, F., Jost, G., Kuznetsov, I., Schneider, B., and Umlauf, L. (2007). Analysis of the water column oxic/anoxic interface in the Black and Baltic seas with a numerical model. *Mar. Chem.* 107, 388–410. doi: 10.1016/j.marchem.2007.06.003

Yang, P., Lee, S., Post, J. E., Xu, H., Wang, Q., Xu, W., et al. (2018). Trivalent manganese on vacancies triggers rapid transformation of layered to tunneled manganese oxides (TMOs): Implications for occurrence of TMOs in low-temperature environment. *Geochimica et Cosmochimica Acta* 240, 173–190. doi: 10.1016/j.gca.2018.08.014

Yu, H., and Leadbetter, J. R. (2020). Bacterial chemolithoautotrophy via manganese oxidation. *Nature* 583, 453–458. doi: 10.1038/s41586-020-2468-5

Zhao, H., Zhu, M., Li, W., Elzinga, E. J., Villalobos, M., Liu, F., et al. (2016). Redox reactions between mn(ii) and hexagonal birnessite change its layer symmetry. *Environ. Sci. Technol.* 50, 1750–1758. doi: 10.1021/acs.est.5b04436

Conflict of Interest: The authors declare that the research was conducted in the absence of any commercial or financial relationships that could be construed as a potential conflict of interest.